PRESSURE-IMPULSE DIAGRAMS USING FINITE ELEMENT ANALYSIS FOR REINFORCED CONCRETE SLABS SUBJECTED TO BLAST LOADING

A THESIS IN
Civil Engineering

Submitted to the Faculty of the University of
Missouri-Kansas City in partial fulfillment of
the requirements for the degree of

MASTER OF SCIENCE

by

Jitesh Kumar Reddy Nalagotla

University of Missouri-Kansas City

2013

PRESSURE-IMPULSE DIAGRAMS USING FINITE ELEMENT ANALYSIS FOR REINFORCED CONCRETE SLABS SUBJECTED TO BLAST LOADING

Jitesh Kumar Reddy Nalagotla, Candidate for the Master of Science Degree,

University of Missouri- Kansas City

ABSTRACT

Reinforced concrete slab systems are widely used in protective structures designed to resist blast events. Blast events subject structures to high pressure and impulse loads. The magnitude of blast load experienced by a structural element is directly related to the exposed area. Hence protection of reinforced concrete slabs and walls, which constitute the maximum exposed area of a structure when subjected to blast loads, is of great importance.

The main purpose of the project is to study the non-linear response of reinforced concrete slabs when subjected to impact and blast loading. Blast loading comprises of impulsive, dynamic and quasi-static loading conditions. And the performance of reinforced concrete slabs subjected to these loads is highly dependent upon the reinforcing steel provided in the slab. Hence a comprehensive analysis is performed on a representative slab panel with varying reinforcement.

Due to the nature of the blast loading analysis method used influences the slab response significantly. Hence the slab response was predicted and compared using finite element (FE) and single degree of freedom (SDOF) methods. An advanced finite element modeling tool, LSDYNA and a commonly used SDOF analysis tool, SBEDS are employed for the purpose of analysis.

A parametric analysis is conducted to develop Pressure-Impulse (PI) curves for different damage levels. Curve fit analysis was performed to characterize the PI curves generated from FE method. Conclusions and future work recommendations are presented for design of reinforced concrete slabs for blast protection based upon the research are presented and discussed.

APPROVAL PAGE

The faculty listed below, appointed by the Dean of the School of Computing and Engineering have examined a thesis titled "Pressure-Impulse Diagrams Using Finite Element Analysis for Reinforced Concrete Slabs Subjected to Blast Loading," presented by Jitesh Kumar Reddy Nalagotla, candidate for Master of Science degree, and certify that in their opinion it is worthy of acceptance.

Supervisory Committee

Ganesh Thiagarajan, Ph.D., P.E., Committee Chair
Department of Civil and Mechanical Engineering

Ceki Halmen, Ph.D.
Department of Civil and Mechanical Engineering

ZhiQiang Chen, PhD.
Department of Civil and Mechanical Engineering

TABLE OF CONTENTS

LIST OF ILLUSTRATIONS

Figure Page

LIST OF TABLES

Table Page

ACKNOWLEDGEMENTS

This is a great opportunity to express my deep and sincere gratitude to my advisor, Dr. Ganesh Thiagarajan, for his continuous guidance, support, and motivation during the last two years. I would also like to thank Dr. Ceki Halmen and Dr. Zhiqiang Chen for serving on the graduate committee.

I would like to mention my lab mates Dr. Yun Kai Lu, Rasek Rahim Zadeh, Kevin Buck and Gunjan Shetye for the fun and memorable moments that we cherished together at the Computational Mechanics lab.

I owe my loving thanks to my parents, RadhaKrishna Reddy Nalagotla, Kalabhashini Nalagotla, my sister Sushmitha Nalagotla and my wife Surekha Reddy Dagimeti for their encouragement, patience, and understanding throughout my studies abroad. I would also like to thank all my family members, in-laws and friends for their loving support.

I gratefully acknowledge the financial support provided by the National Science Foundation for this research thesis.

CHAPTER 1

INTRODUCTION

Reinforced concrete has been a widely used construction material in protective structures. There are several alternatives in material and framing of building structures designed for gravity, wind or seismic loads. However reinforced concrete has been primarily used for floor and wall construction of protective structures due to serviceability, ductility and strength performance of the material when subjected to extreme dynamic loads such as blast loads.

Structures are usually designed for linear-elastic response when subjected to sustained loads such as gravity and wind loads. Blast and seismic loads subject structures to a non-linear response. The non-linear response of a structure can be at three levels namely, (1) material (2) structural element and (3) structure. It is important to characterize the non-linear response of reinforced concrete structural members when subjected to extreme dynamic loads with a reasonable confidence. This thesis characterizes the behavior of one way reinforced concrete (RC) slabs subjected to blast loading.

Blast loading can be broadly categorized into three types namely, (1) impulsive loading (2) dynamic loading and (3) quasi-static loading depending on the proximity and intensity of explosion. An RC slab in a protective structure can be subjected to any of the above mentioned blast loading regimes depending on the charge weight and standoff distance of the explosive used. It is evident that it can be very expensive to determine the nonlinear response of RC slabs for the whole range of blast loading using experimental data.

However, the response of RC slabs to these varieties of loadings can be effectively captured using Pressure-Impulse (PI) curves which can be further validated using experimental data.

PI curves are a type of response spectra developed for structural elements subjected to blast loading. PI curves are specific to the material and sectional properties of the structural element. PI curves are also called iso-damage curves as they represent the combinations of pressure and impulse values that cause a specified damage level in the structural element. The pressure and impulse values depend on the charge weight and standoff distance of the explosive used. While the pressure considered in PI curves is the peak pressure the structural element is subjected to due to explosion, the impulse is the area of the region bound by the time history curve of the pressure applied. Damage level typically corresponds to the maximum inelastic deformations that occur in the RC slab due to blast loading.

1.1. Problem Statement

Analysis methods ranging from single degree of freedom (SDOF) methods to advanced numerical methods such as finite element (FE) methods have been typically used to develop PI curves for various structural elements in a protective structure. The blast analysis of RC slabs can be performed based on the response of a single degree of freedom (SDOF) elastic-plastic structure and the link between the duration of the blast load and the natural period of the vibration of the structure(Mays and Smith 1995). SDOF modeling is a simple and efficient method and realistically represents the structural behavior based on the anticipated mode of response. However, SDOF analysis of a structure subjected to blast loading has its own disadvantages. The use of SDOF model may not be suitable for

structural damage analysis to due to blast loads because damage may be governed by the local modes of the structure, especially when the loading is impulsive(Karthaus and Leussink 1983).

Hence SDOF analysis methods are easy and simple to use but have their inherent limitations on the kinds of failure modes that they can capture. On the other hand, FE methods are capable of incorporating complex features of the material behavior, slab geometry and boundary conditions. LS-DYNA(2010), as a finite element program capable of performing non-linear dynamic analysis, has several material models for concrete that were developed by researchers for different applications. Developing PI diagrams using LS-DYNA is a time consuming procedure requiring numerous simulations to develop PI diagram for each different structural element and each damage level. However, this software program is used extensively in research projects to simulate the blast loading of structures and the structural response due to the availability of advance material models and the validation of these material models with experimental data.

The reinforcement ratio in an RC slab has a primary effect on the non-linear response. PI curves provide an efficient way to compare the performance of reinforced concrete slabs with varying reinforcements. In this study, we develop and compare PI curves using SDOF and FE methods for RC slabs with varying reinforcement ratios subjected to the three regimes of the blast loading. The PI curves developed are further compared with experimental and design values and curve fit analysis is used to characterize the pressure impulse relationship for each damage level.

1.2. Objective of the Study

This study has the following five objectives:

1) Perform a parametric study using SDOF and FE methods to develop pressure-impulse diagrams for a reinforced concrete slab in order to study the effect of longitudinal reinforcement ratio, rebar size and spacing on the reduction of damage level at impulsive, dynamic, and quasi-static loading conditions.
2) Compare and study the non-linear response of the above reinforced concrete slabs analyzed with finite element and single degree of freedom methods.
3) Perform curve fit analysis to characterize the pressure-impulse diagrams generated from the finite element method.
4) Compare the numerical PI diagrams with experimental data for validation and with design examples using applicable code of practice for blast design of RC structural elements.
5) Research prevalent seismic detailing practices and study it's applicability to blast response of reinforced concrete slabs.

1.3. Scope of the Study

In order to accomplish the objectives outlined above, the following tasks are performed:

1. Generate finite element model of a reinforced concrete slab panel with four different reinforcement ratios with two rebar sizes and two rebar spacing
2. Numerically subject the slabs to explosions with different standoff distance and charge weights or pressure loads, and generate pressure-impulse diagrams by using maximum structural response for a given applied pressure and impulse loading

3. Compare the pressure-impulse diagrams for the four slabs developed with finite element and single-degree of freedom methods
4. Perform curve fit analysis of PI Curve data from FE analysis to develop equations for pressure-impulse diagrams.
5. Validate the curve fit equations by comparing with pressure-impulse diagrams developed using finite element methods
6. Compare the developed PI curves with experimental values and design examples using applicable code of practice for blast design
7. Study prevalent seismic detailing practices of reinforced concrete slabs and it's applicability to blast response

1.4. Thesis Organization

This thesis is organized into the following four chapters:

- Chapter 2: Discusses the dynamic analysis of reinforced concrete slabs using single and multiple degrees of freedom analysis and briefly describes the experimental program
- Chapter 3: Discusses the pressure impulse diagrams developed using methods described in chapter two and use of curve fit analysis on FE PI Curve data to develop equations to characterize PI Curves for reinforced concrete slabs with four types of longitudinal reinforcement
- Chapter 4: Discusses the comparison of PI curves developed in previous chapter with experimental values and design examples using applicable code of practice. This

chapter also discusses the seismic detailing of reinforced concrete slab and it's applicability to blast response

- Chapter 5: Provides conclusions of this study and recommendations for future work

CHAPTER 2

BLAST RESPONSE OF REINFORCED CONCRETE SLABS

An explosion is defined as a large-scale, rapid and sudden release of energy. The detonation of a condensed high explosive generates hot gases under pressure. The hot gas expands forcing out the volume it occupies. As a consequence, a layer of compressed air (blast wave) forms in front of this gas volume containing most of the energy released by the explosion. Blast wave instantaneously increases to a value of pressure above the ambient atmospheric pressure. The blast impulse is the area under the pressure-time curve. The pressure-impulse (PI) curve is an easy way to mathematically relate a specific damage level to a combination of blast pressures and impulses imposes on a particular structural element.

In order to develop PI diagrams for a structure using SDOF analysis, the calculation of the final state of the structure rather than a detailed knowledge of its displacement time-history is the principal requirement. The principles of this analysis can be established based on the response of a single degree of freedom (SDOF) elastic-plastic structure and the link between the duration of the blast load and the natural period of the vibration of the structure(Mays and Smith 1995). A SDOF model of a structure is constructed based on the dominant response mode of a structure which is normally responsible for the overall structural failure. Equivalent mass, damping, and stiffness are the parameters used to describe a SDOF model(Krauthammer 1998). Since SDOF modeling is simple, efficient and realistically represents the structural behavior based on the anticipated mode of response, it is a useful tool to predict the overall response of a structure, which determines the damage level of a structural system or structural element(Li and Meng 2002).

However, SDOF analysis of a structure subjected to blast loading has its own disadvantages. The use of SDOF model may not be suitable for structural damage analysis due to blast loads because damage may be governed by the local modes of the structure, especially when the loading is impulsive(Karthaus and Leussink 1983).

Finite element modeling allows using sophisticated concrete material models that provide more accurate representation of the actual response of concrete. Modeling the steel reinforcements as discrete elements using separate material models while coupled with concrete elements also improves the accuracy of the results.

2.1. Literature Review

Criswell(1972) conducted static and dynamic tests on a ¼ scale prototype shelter consisting of a reinforced concrete slab system to resist a 15 psi air blast overpressure loading. The empirical methods used to design the slab were modified to include dynamic loading effects. Agardh(1997) performed blast experiments in a shock tube on steel fibre reinforced and conventionally reinforced concrete slabs to validate finite element codes and material modeling including the Winfrith(Broadhouse 1995) model of LS-DYNA(2010). The research concluded that the simulations give fairly accurate estimate of displacements for low loads and the strain rate was observed not to be significant due to the large distance between the slabs and the charges(Agardh 1997).

Krauthammer and Otani(1997) performed intensive numerical simulations to study the effect of various parameters like reinforcement details, finite element mesh size and some loading conditions. The results from above simulations were analyzed to present recommendations that could assist efficient numerical simulations (Krauthammer and Otani

1997). Mlakar et al. (1998) analyzed the blast damage to the Murrah Building in Oklahoma city due to a vehicular bomb attack, which destroyed three columns and floor slabs in the vicinity of the blast. The calculated peak over-pressures varied from a maximum of over 69 MPa (10,000 psi) at the point closest to the detonation to a minimum of 62 kPa (9 psi) (Mlakar Sr, Corley et al. 1998).

Biggs et al.(2000) used finite element modeling capabilities of ABAQUS to analyze reinforced concrete bridge decks for effective depiction of the nonlinear behavior of concrete. Low and Hao(2002) formulated an equivalent SDOF system to study the reliability of a reinforced concrete slab with variations in material strength, slab thickness, percentage of reinforcement and support conditions. Mosalam et al.(2001) developed computational models for reinforced concrete slabs with and without CFRP composite strips and verified the models using static experiments. It was observed that the improved slab behavior with the CFRP composite slab system is best when retrofitting is applied to both sides of the slab.

Low and Hao(2002) also formulated two loosely coupled SDOF systems to represent the flexural and direct shear modes. The numerical results indicated that a slab tends to fail in direct shear mode if the blast load amplitude is high but of short duration and it tends to fail in flexure failure mode if load amplitude is relatively low and duration is relatively long. Bogosian et al.(2002) compared blast load predictions from a number of popular simplified models to a wide range of test data spanning three decades and comprising a total of nearly 300 individual measurements. Li and Meng(2002) conducted a fundamental study of the pressure impulse diagram for various descending pulse loads based on dimensional analysis and a SDOF model. It was found that the effect of pulse loading shape on the pressure impulse diagram was considerable.

Georgin and Reynouard(2003) used numerical simulations to conclude that concrete behavior would have to be considered as viscoelastic to improve the model prediction. Krauthammer et al.(2003) developed a modified SDOF computer code that appears to follow closely the trend of experimental data. Morison(2006) reviewed SDOF methods for dynamic analysis of reinforced concrete flexural members subjected to blast loading. It was observed that the widely published parameters in common usage for two-way spanning members such as slabs and walls are inaccurate by almost up to 50% for some coefficients. Zineddin and Krauthammer(2007) conducted experimental studies to study the dynamic response and behavior of reinforced concrete slabs under impact loading. The test data indicated that the amount of steel reinforcement affected the response of slab and particularly the slab failure modes.

Hao and Zhongxian(2008) numerically investigated the influence of concrete strength, thickness and reinforcement ratio on the behavior of reinforced concrete slab under blast loading. One loading case with charge weight of 1000 Kg TNT and 10 m standoff distance was considered for the above simulations. Schenker et al.(2008) conducted full scale field explosion tests on protected and unprotected concrete slabs. Simulation of the concrete slab response to the blast wave load showed a complex behavior of “spring back” due to insufficient restrain of the slab edge. Yuan et al.(2008) conducted numerical simulations of concrete slabs subjected to different contact detonation. It was concluded that some measures can be taken to optimize the arrangement of reinforcing bars so as to strengthen the anti-spallation capability of concrete structures.

Zhou et al.(2008) used a dynamic plastic damage model for concrete material to estimate responses of both an ordinary reinforced concrete slab and a high strength steel

fibre concrete slab subjected to blast loading. The interaction between the blast wave and concrete slab was also considered in 3D simulation. Hao and Zhongxian(2008) used the above model to perform numerical simulations of exterior reinforced concrete wall for several blast loadings. Analytical formulae were derived from above simulations for a quick assessment of the RC wall performance under blast loadings.

Tanapornraweekit et al.(2007) presented blast test results on a reinforced concrete slab panel with 5000 Kg TNT at 40 m standoff. Finite element numerical analysis was also conducted and the study showed only 17% difference in maximum deflection compared to the observed value. Krauthammer et al.(2008) described theoretical and numerical methods for deriving pressure impulse diagrams for structural elements subjected to transient loads. It was observed for the cases where the resistance function is nonlinear and/or the load pulse is irregular, numerical solutions are the only reasonable means for deriving pressure impulse diagrams.

Jones et al.(2009)proposed a finite difference method for the analysis and design of simply supported structural members subjected to blast loads. A comparison between the measured and analytical responses was made and the largest difference was observed to be only 21%, indicating that the finite difference analysis model can accurately predict the response of a simply supported structural member to blast loads. Kuang et al.(2009) compared blast test results of a reinforced concrete slab with finite element numerical analysis using LS DYNA and concluded that the numerical simulation is an appropriate way for the study of responses of reinforced concrete components under blast load. Sangi and May(2009) performed finite element analysis of reinforced concrete slabs under drop-weight impact loads using LS DYNA.

Wu et al.(2009) carried out a series of blast tests to investigate the blast resistance of reinforced concrete slabs. Evaluation of pressure histories showed that the use of end-detonated cylindrical charges will produce shock fronts in the near field that differ substantially from those assumed in TM5-1300(1990) for standard blast design. Razaqpur et al.(2009) critically discussed the fundamental concepts used for evaluating the flexural and axial resistance structures under blast. It was concluded that the structural response to a blast event cannot be determined accurately using SDOF methods since structural nonlinearities and strain rates can alter the structure stiffness, strength and ductility dramatically. Hussein(2010) studied the non-linear analysis of SDOF system subjected to blast loading.

El-Dakhani et al.(2010) used a SDOF model based on the guidelines of UFC 3-340-02(Polcyn and Myers 2010) to generate pressure impulse diagrams and compared to the results of experimentally validated nonlinear explicit FE analysis of two way slabs. It was concluded that the deficiencies in the SDOF resistance functions included strength underestimation resulting from neglecting multiple yield line patterns and corner effects.

PI curves are characteristic to the material and sectional properties of the structural element and also dependent upon damage level of the structural element. Robert et al.(2008) performed dynamic testing of ten 1/3 scale reinforced concrete slabs using the Blast Load Simulator (BLS) at ERDC-Vicksburg. The primary objective of this research is to estimate the blast response of the above 1/3 scale panels to all possible loading conditions by developing PI curves using FE and SDOF methods.

2.2. Reinforced Concrete Slabs Subjected to Blast Loads

Reinforced concrete is a commonly used material in construction of protective structures. The safety of these structures subjected to blast and impact loads has been one of the primary concerns for designers in recent years. In the design of buildings to resist the effects of blast loading or other severe dynamic loads, it is not economical to consider the structural response in its elastic range only. Therefore, the structural elements should be allowed for certain plastic deformations, which better utilizes their energy absorbing capabilities if exposed to dynamic loads.

An explosion is a result of a sudden release of energy. An explosion in air creates a blast wave as a result of the large accumulation of energy pushing back the surrounding atmosphere. This wave moves outward from the central part only a fraction of second after the explosion occurs. The front of the wave called the shock front, is like a wall of highly compressed air and has an overpressure much greater than that in the region behind. This first part of the blast wave is termed the positive phase. Then, the pressure will continue to decay below the ambient pressure until the minimum negative pressure is reached, after which the ambient pressure is obtained once more. The second part of the blast wave is termed the negative phase and usually exhibits a longer duration than that of the positive phase. In design, the negative phase is normally less important compared to the positive phase. However, in some cases it is important to also consider the effects of the negative phase, e.g. when considering damage of windows or in a case with heavy structures having a response time longer than the positive phase. An ideal blast-wave profile is in figure 2-1.

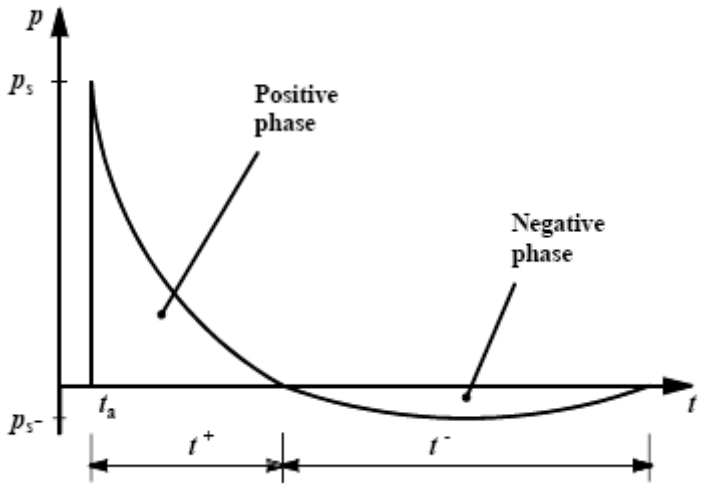

Figure 2-1: Ideal blast-wave profile

The behavior of structures that are subjected to rapidly changing loads may change significantly from that under static or quasi-static situations. Common for all dynamic events of a structure is the presence of inertial effects due to accelerating masses. Due to the inertial effects the elements that comprise the structure will try to resist any change in velocity and these effects need to be considered in a dynamic analysis. The analysis of the dynamic response of reinforced concrete slabs under blast loading is complicated due to the fact that the impulsive load caused by an explosion is highly nonlinear and occurs in an extremely short duration compared to the fundamental period of the structure or structural element. The duration of blast pressure is significantly important along with its magnitude for dynamic response of concrete elements.

Reinforced concrete slabs subjected to air blast loading can fail in a variety of mechanisms. They can fail in flexure where plastic hinges form at locations where the ultimate bending moment capacity is obtained, i.e. at mid-span for a simply supported slab where a symmetric load is applied. For this failure mode, initial cracking of the concrete is followed by subsequent yielding of the tensile reinforcement. However, the initial flexural

cracks can also be followed by the formation of inclined diagonal tension cracks. This is called flexural shear failure and is abrupt and brittle in nature. In addition to the above two failure modes, slabs can also fail in direct shear mode at the supports. This is characterized by the rapid propagation of vertical cracks through the depth of the element. The brittle and ductile response of a reinforced concrete slabs are illustrated in figure 2-2 and figure 2-3.

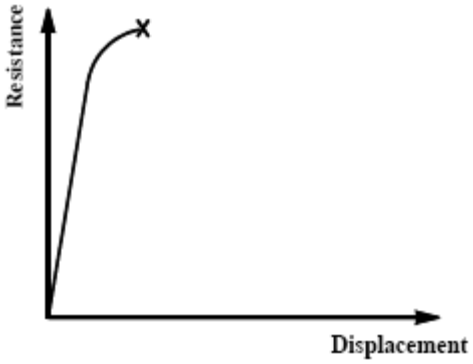

Figure 2-2: Brittle response of a reinforced concrete slab

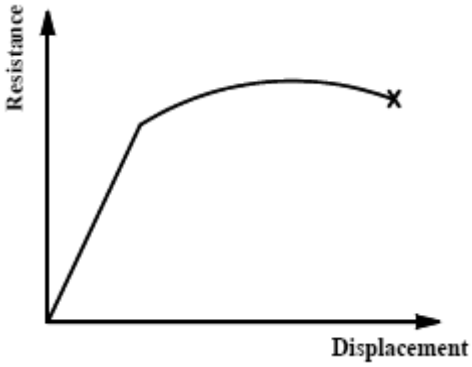

Figure 2-3: Ductile response of a reinforced concrete slab

2.3. Dynamic Material Properties

Blast load durations are generally milliseconds, causing component response times to be similarly short durations. Reinforced concrete structures subjected to blast loading will respond by deforming over a relatively short period of time and the strain rates in the

concrete and reinforcement reach magnitudes considerably higher than that of a statically loaded structure. Therefore, the effects of dynamic material properties should not be ignored. Under dynamic loads, materials exhibit increased yield strengths due to strain rate effects, which can considerably improve the ultimate load capacities of blast-loaded components. The material strength increase is normally referred to as a dynamic increase factor (DIF), which is the ratio of the dynamic to the static value. The elastic modulus of concrete is also affected by changes in strain rate.

Similarly to concrete, steel reinforcement bars are also affected by dynamic loads and will exhibit different degrees of strength increases depending on steel grade. Both the yield strength and ultimate strength increase, but the increase of the former is usually more significant. There is difference between actual reinforcing steel static yield strengths and the minimum specified values obtained from many tensile tests. Hence the minimum specified yield strength for reinforcing steel *fy* is typically increased by a static increase factor (SIF) for blast design to account for the difference.

2.4. Single Degree of Freedom Systems

A single degree of freedom system is one in which only one coordinate is essential to define its motion. The simplest vibratory system can be described by a single mass connected to a spring (and possibly a dashpot). The mass is allowed to travel only along the spring elongation direction. Such systems are called *Single Degree-of-Freedom* (SDOF) systems and are shown in the following figure 2-4.

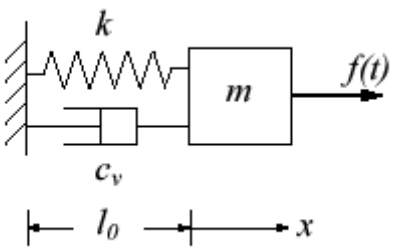

Figure 2-4: Single degree of freedom system (SDOF)

The basic differences between structures under static and dynamic loads are the presence of inertia in the equation of motion and that of kinetic energy in the equation of energy conservation. Both terms are related to the mass of the structure and, hence, the mass of the structure becomes an important consideration in dynamic analysis. Structural elements can in many cases be reduced to an equivalent dynamic system having a similar behavior as the real element.

Protective design manuals ((DoD) 2007) use two common SDOF modeling approaches: the modal method and the equivalent SDOF method. In the modal method, the elastic forced response of a member is approximated by the first mode of free vibration. In the Equivalent SDOF method, before analyzing the response of a structural element with distributed mass and loading; the mass, resistance and loading are replaced in Newton's equation of motion with the equivalent values for a lumped mass-spring system. The equivalent SDOF method is widely used in protective design practices. The ultimate dynamic moment capacity is calculated using applicable DIF and SIF factors for reinforcing steel and concrete without any strength reduction factor. It is intended to be a realistic estimate of the actual dynamic moment capacity at the maximum moment regions of the component. Yield line theory is used to determine the ultimate resistance for indeterminate components. An idealized resistance deflection curve using SDOF method is illustrated in

figure 2-5. K_{L1} and K_{L2} in the figure 2-5 represent equivalent stiffness for elastic and elastic-plastic regions. The resistance deflection curve used in protective design manuals follows the same pattern.

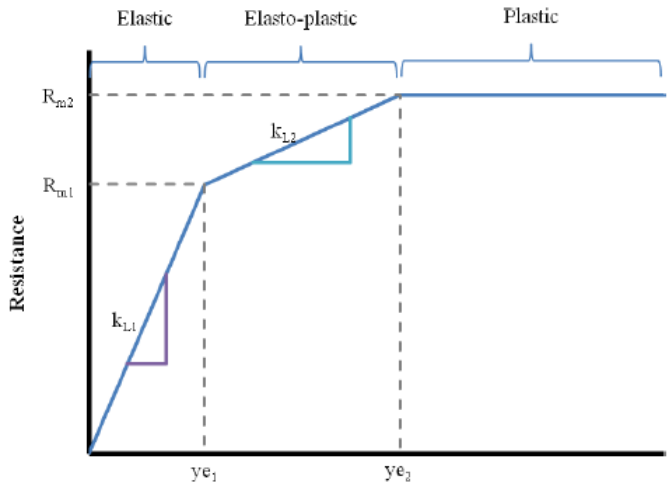

Figure 2-5: Resistance deflection curve using SDOF method

SBEDS(2008) is an Excel-based tool used to perform Single-Degree-of-Freedom (SDOF) dynamic analyses of structural components subjected to blast loads. It was developed for the U.S. Army Corps of Engineers Protective Design Center to meet Department of Defense Antiterrorism standards((DoD) 2007).

2.5. Multiple Degree of Freedom Systems

Rigorous analysis methods using multiple degree of freedom systems and numerical methods may be used to obtain the dynamic response considering more-complex effects. The numerical methods most appropriate to the simulation of the blast problem are typically based upon a finite difference, or finite element method using explicit time integration techniques. In recent years, several constitutive material models were developed for prediction of more accurate behavior of concrete and steel reinforcement. In blast scenarios,

structural components might deform in high order modes and be damaged locally under blast load. Therefore, the simplified SDOF system can′t accurately represent the structural component. The combined shear and flexural damage mode is also very likely to occur, in which case the maximum deflection related damage criterion will also fail to assess the damage level of structural components under blast load.

Advanced finite element methods provide the best analytical results because they can take into account the time varying load, dynamic structural response, non-liner material properties, and the non-linear interaction of various response modes (e.g., shear and flexure). LS-DYNA(2010) is a unique advanced finite element method that offers the analyst the choice of Lagrange, Eulerian(ALE) and Simple Engineering solvers, and combinations of these solvers, for simulating high energy events such as blast loading. To realistically predict the behaviors of reinforced concrete structures under various types of loads, the concrete constitutive model needs to be shown to simulate known behaviors at smaller specimen levels up to the full-scale structural level. LS-DYNA provides several constitutive models for concrete. The Winfrith Concrete Model(Broadhouse 1995) of LS-DYNA used in this research, also called the smeared crack model was originally developed in response to the requirement of the nuclear industry for a finite element analysis capability to predict the local and global response of reinforced concrete structures subjected to explosive and impact loadings.

2.6. Experimental Study and Design of RC Slabs

An experimental investigation on which this research study is based upon, was done on twelve 1/3 scale reinforced concrete slabs with single mat reinforcement. The

experiments were performed by Dr. Ganesh Thiagarajan, Principal Investigator for this project, at the U.S. Army Engineering Research and Development Center, Vicksburg, MS. The experimental study is not a part of this research thesis but the experimental data was compared with analytical results of SDOF and FE analysis performed in this research study for validation. Unified Facilities Criteria Code UFC 3-340-02(Polcyn and Myers 2010) prescribes design of reinforced concrete slabs for blast loads. The comparisons of experimental and design values with PI curves developed analytically in Chapter 3 are discussed in detail in Chapter 4.

CHAPTER 3

PRESSURE-IMPULSE DIAGRAMS FOR REINFORCED CONCRETE SLABS

This chapter presents the development of pressure impulse (PI) curves for four slab models using single and multiple degrees of freedom methodologies. Single degree of freedom methodology is employed using SBEDS(2008), an EXCEL based tool developed for the U.S Army Corps of Engineers Protective Design Center. The multiple degree of freedom methodology is employed using advanced finite element software, LS-DYNA(2010). The pressure impulse curves developed using the above methods are compared for the four slabs and a multiple regression analysis is performed to derive equations to predict pressure impulse curves.

3.1. Development of Pressure-Impulse Curves

The pressure impulse diagrams as iso-damage curves include three regimes: impulse-controlled, dynamic and pressure controlled regimes. These regimes are illustrated in Figure 3-1 as regimes I, II, and III respectively(Li and Meng 2002). To identify blast loading conditions that fall in each regime, Smith et al.(2009) used the scaled distance Z, which is defined as the ratio of the standoff distance to the cubic root of the charge weight. The response regime is categorized as follows (Smith, McCann et al. 2009):

Close in: $Z < 1190$ mm/kg$^{1/3}$ ($Z < 3$ ft./lb$^{1/3}$)

Near Field: $1190 < Z < 3967$ mm/kg$^{1/3}$ ($3 < Z < 10$ ft./lb$^{1/3}$)

Far Field: $Z > 3967$ mm/kg$^{1/3}$ ($Z > 10$ ft./lb$^{1/3}$)

The close-in (region I) regime is associated with the impulsive type of loading while in the far field (region III) regime the loading becomes quasi-static and pressure controlled.

In the near field regime (region II) both the pressure and impulse affect the response of the structure.

Damage Criterion: Each pressure impulse curve represents a damage level that the structural element experiences due to the various blast loading conditions. For this study, the ratio of the commonly used mid-span displacement to the effective span of the slabs is considered as the damage criterion. For each simulation, the maximum displacement of the central node at the mid-span cross section of the slab is read from LS-DYNA's output. After running multiple simulations and following the procedure described above, the points whose damage levels are the same are connected to form a damage level curve, called the pressure impulse diagram for the specific level of structural damage.

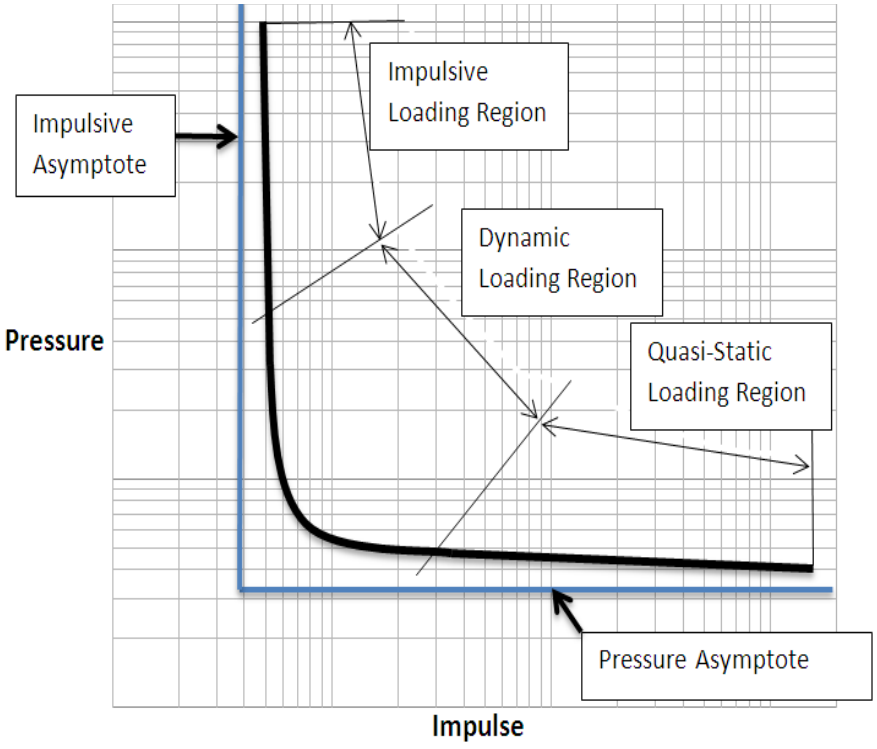

Figure 3-1: A typical Pressure-Impulse diagram

Significance of PI curve: Each PI curve represents a damage level that a structural element experiences due to the various blast loading conditions. Hence a blast load combination with pressure and impulse coordinate which is below the PI curve is considered to cause less damage to the structural element than the damage level the PI curve represents. And a blast load combination with pressure and impulse coordinate which is above the PI curve is considered to cause more damage to the structural element than the damage level the PI curve represents. Here, the blast load combination refers to a charge weight and standoff distance and the damage level typically used in RC slabs is the maximum inelastic deflection the RC slab experiences due to blast load. Hence any combination of pressure and impulse which falls below the PI curve is considered to be a conservative. However, it is also important to note that the PI curve itself is considered conservative if it falls below the experimental pressure and impulse values for the observed deflection corresponding to the damage level of the PI curve.

3.2. Analysis Methods

Single and multiple degree of freedom analysis are the two most common approaches used to analyze structures for blast effects. Single degree of freedom methods are commonly used in both design and research applications. Multiple degree of freedom methods are traditionally used in research applications. This is mainly due to the time required to use these methods to provide guidance for the design of structures for blast loads. However, when using simplified approaches it is important to be conservative in order to design safe structures. The effects of dynamic loads such as blast loads are complicated and hence it is important to verify and validate the performance of simplified approaches with more robust and accurate methods. SBEDS(2008) is a widely used single degree of

freedom analysis tool for blast response and LS-DYNA(2010) is advanced finite element software improved over several years to give a closer estimate of blast effects on structures. Hence these two methods are employed in this study.

3.3. Material Models in LS-DYNA

LS-DYNA(2010) is an advanced finite element software program which is used to simulate the response of structures to blast and impact loading. Several numerical blast analyses work with an explicit non-linear dynamic finite element code LS-DYNA has been reported in literature. Several material models are available in LSDYNA. In this research study, the Winfrith Concrete Model(Broadhouse 1995), material type 84in LS-DYNA, has been chosen to model the concrete in the single mat RC slabs to be consistent the available parameter input strength got both high-strength and normal-strength concrete (study involving high-strength concrete is not part of this thesis and hence not presented here). The steel is modeled using the Plastic Kinematic model(LSDYNA_971 2010), material type 003 in LS-DYNA and the interface between the steel and concrete is defined using *CONSTRAINED_LAGRANGE_IN_SOLID(LSDYNA_971 2010) formulation.

3.3.1. Winfrith Concrete Model

The Winfrith Concrete model is a smeared crack (pseudo crack) model developed by Broadhouse(1995) over many years and has been validated against experiments. The Winfrith Concrete model is implemented in the 8-node single integration point continuum element. The Winfrith Concrete model in LS-DYNA uses a basic plasticity model based upon the shear failure surface developed by Ottosen(1977). The shear surface expands with increasing hydrostatic stress, and its radii at the compressive and tensile meridian are

determined by locally rate sensitive compressive and tensile strengths as documented by Broadhouse(1995). The basic plasticity model is referred to as a four parameter model in which the first two parameters denoted by constants *a* and *b* represent the meridional shape of the shear failure surface and the second two parameters denoted as k_1 and k_2 define the shape of shear failure surface in the octahedral plane (π-plane)(Schwer 2011). The failure surface is described analytically as a function of stress tensor and stress deviator tensor as shown in equation 1:

$$F(I_1, J_2, \cos 3\theta) = a\frac{J_2}{(f'_c)^2} + \lambda\frac{\sqrt{J_2}}{f'_c} + b\frac{I_1}{f'_c} - 1$$

……..…Equation 1

The constants '*a*' and '*b*' depend on the ratio of unconfined tensile strength to the unconfined compressive strength and control the meridional shape of the shear failure surface. The function $\lambda = \lambda\cos(3\theta)$ is defined in the π-plane shape factors as shown in Equation 9 with $-1 \le \cos 3\theta \le +1$ for triaxial compression to triaxial compression and controls the shape of shear failure surface on the π-plane. In the Winfrith concrete model, the invariants of the stress tensor are calculated first and then the invariants of the deviatoric stress tensor are computed using identities.

The stress tensor, σ_{ij} has three scalar invariants (Eigenvalues):

$$I_1 = \sigma_{kk}$$

$$I_2 = 0.5(\sigma_{ii}\sigma_{jj} - \sigma_{ij}\sigma_{ji})$$

$$I_3 = DET(\sigma_{ij})$$

……..Equation 2

The first invariant of the stress tensor, $I_1 = \sigma_{kk} = 3P$ and P is the mean stress. The meridional shape parameters 'a' and 'b' are calculated internally in the Winfrith model using three non-dimensional constants, $\alpha = 1.16; \beta = 0.5907445; \gamma = -0.6123724$ as per equation 3:

$$b = \frac{1 + R\alpha\frac{\gamma}{3} - \alpha^2\frac{\gamma}{3} - \frac{\alpha}{R}}{\alpha^2\frac{\beta}{3} - 3\alpha - R\alpha(\frac{\beta}{3})}$$

$$a = \beta b + \gamma$$

……Equation 3

Here, $R = \frac{f'_t}{f'_c} \leq 1$ is the ratio of unconfined tensile to compressive strength. The deviatoric stress tensor, S_{ij} is introduced to separate the mean stress from the shear response as shown in equation 4:

$$S_{ij} = \sigma_{ij} - \frac{\sigma_{kk}}{3}$$

…...……Equation 4

The first two invariants of the deviatoric stress tensor, J_2 and J_3 are as given in equation 5:

$$J_1 = S_{kk} = S_{11} + S_{22} + S_{33}$$

$$J_2 = 0.5 S_{ij} S_{ij} = \frac{1}{3} I_1^2 - I_2$$

$$J_3 = DET(S_{ij}) = \frac{2}{27} I_1^3 - \frac{1}{3} I_1 I_2 + I_3$$

……Equation 5

The third invariant of the deviatoric stress tensor is represented as an angle (Lode Angle, θ with limits $0 \le \theta \le \frac{\pi}{3}$) in the π – plane is defined in equation 6:

$$\cos 3\theta = \frac{3\sqrt{3}}{2}\frac{J_3}{J_2^{1.5}}$$

…..…….Equation 6

Two additional constants are defined in the Winfrith model in terms of constants '*a*' and '*b*':

$$c = \frac{\sqrt{3}}{R}(1 - bR - R^2\frac{a}{3})$$

$$d = \frac{3 + 3b - a}{\sqrt{3}}$$

……Equation 7

The π – plane shape factors in terms of constants *c* and *d* are as shown in equation 8:

$$k_2 = \cos[3\tan^{-1}(\frac{1}{\sqrt{3}} - \frac{2d}{c\sqrt{3}})]$$

$$k_1 = \frac{c}{\cos[\frac{1}{3}\cos^{-1}(k_2)]}$$

…..…….Equation 8

The function $\lambda = \lambda\cos 3\theta$ is now defined in terms of the constants k_1 and k_2 as shown in equation 9:

$$\lambda = k_1\cos[\frac{\cos^{-1}(k_2\cos 3\theta)}{3}] for \cos 3\theta \ge 0$$

$$\lambda = k_1\cos[\frac{\pi}{3} - \frac{\cos^{-1}(-k_2\cos 3\theta)}{3}] for \cos 3\theta \le 0$$

...……Equation 9

The four parameters a, b, k_1 and k_2 thus define the shear failure surface in the Winfrith concrete model(Schwer 2011). The uniaxial compressive and tensile strengths along with mass density, initial tangent modulus, Poisson's ratio are provided as input parameters in the Winfrith concrete model. The input parameters used in this research study are shown in Table 3-1. Typical concrete material properties used in the FE analysis are also shown in figure A-1 of Appendix A.

Table 3-1: Input variables in *MAT_WINFRITH_CONCRETE

Variable	Description	Input Value
RO	Mass Density	2.246E-04 lbs.-s/in^3
TM	Initial Tangent Modulus of Concrete	3.6E+06 psi
PR	Poisson's Ratio	0.18
UCS	Uniaxial Compressive Strength	4000 psi
UTS	Uniaxial Tensile Strength	475 psi

The hydrostatic stress state in the concrete is determined from a typical non-dimensionalized volume compaction curve determined by Broadhouse(1995). The volume compaction curve is a pressure-volumetric strain curve, defined by the derived strain and pressures occurring at the unconfined compressive strength, f'_c. If the strain and pressure values are not defined by user, the Winfrith model generates strain and pressure values as per equation 10:

$$P_c = \frac{f'_c}{3}$$

$$K = \frac{E_s}{3(1-2\nu)}$$

…….Equation 10

Here, P_c is the pressure at uniaxial compressive failure, K is the bulk modulus, E_s is the input tangent modulus and ν is the Poisson's ratio. For normal strength concrete used in this research study:

$$P_{c4000psi} = \frac{f'_c}{3} = \frac{4000}{3} = 1333.33psi = 9.19Mpa$$

$$K = \frac{E_s}{3(1-2\upsilon)} = \frac{3.6E+06}{3*(1-2*.18)} = 1.875E+06psi = 12927Mpa$$

The Winfrith model generated Volume Compaction curve for the 4000 psi compressive strength concrete model used in this research study is shown in table 3-2.

Table 3-2: Volumetric Compaction curve in *MAT_WINFRITH_CONCRETE

Volumetric Strain	**Pressure**	**Pressure (x*Pc)**	
$-P_c/K$	**x**	**psi**	**Mpa**
-1.900E-5	1.33	1774	12.23
-0.002000	2.00	2667	18.39
-0.004000	4.00	5333	36.77
-0.010000	6.40	8533	58.84
-0.020000	8.00	10667	73.54
-0.030000	10.00	13333	91.93
-0.041000	12.60	16780	115.83
-0.051000	15.39	20520	141.48

The Winfrith concrete model in LS-DYNA offers two strain rate options via the user input parameter RATE. The user can include the strain rate in the model by specifying RATE = 0 or exclude the strain rate in the model by specifying RATE =1. The reliability of the results when strain rate is included in Winfrith model is not considered to be reasonable as observed by Agardh(1997), the strain rate is not included in this current research.

3.3.2. The Plastic Kinematic Model for Steel

The Plastic Kinematic model(LSDYNA_971 2010) (material type 003) is a bilinear elastic plastic material model that contains formulations containing isotropic and kinematic hardening. Only kinematic hardening, which is expected behavior of reinforcement can be considered by setting the parameter, BETA =0. Strain rate can also be accounted for using Cowper and Symonds model which scaled the yield stress with a factor. For this material, the mass density used is 7.3×10^{-4} lb/in^3, Modulus of Elasticity is 2.9×10^7 psi, Poisson's ratio is 0.30 and Yield Stress is 60,000 psi. The reinforcing steel material properties used for FE analysis in this project are also shown in figure A-2 of Appendix A. In order to couple concrete and reinforcement in the model, an LS-DYNA command called *Constrained_Lagrange_In_Solid(LSDYNA_971 2010) is used. The reinforcement is introduced as the slave elements and concrete as the master.

3.3.3. Constrained Lagrange in Solid Formulation

In order to achieve good interaction between concrete and steel elements, a proper coupling mechanism needs to be used. In this study, the reinforcement is modeled in a discreet manner as shown in Figure 3.2. There are various ways to achieve coupling in LSDYNA such as merging the reinforcing beam elements with solid concrete elements in the form of shared nodes. Secondly, the beam elements can be tied to the concrete elements using 1-D contact which accounts for bond-slip between concrete and steel. Since the loads under consideration are that of explosive in nature and the rate of loading is very high, bond-slip can be neglected for blast and impact studies. Furthermore, the reinforcing beam elements can be coupled to concrete elements through the

CONSTRAINED_LAGRANGE_IN_SOLID* formulation.** This method when used with the fluid-structure coupling mechanism of CTYPE = 2, couples concrete with reinforcement in an efficient manner and it removes the burden of having to align the beam nodes to the solid element nodes.

3.4. SBEDS Analysis Methodology

The SBEDS(2008) workbook is an EXCEL-based tool for design of structural components subjected to dynamic loads using single degree of freedom (SDOF) methodology. It was developed by the U.S. Army Corps of Engineers Protective Design Center as a tool for designers to use in satisfying Department of Defense (DoD) antiterrorism standards((DoD) 2007). Reinforced concrete slabs subject to blast loads are modeled as an equivalent SDOF mass-spring system with a non-linear spring. The mass and dynamic loads of the equivalent system are based on the component mass and blast load, respectively, and the spring stiffness and yield load are based on the component flexural stiffness and lateral load capacity. The properties of the equivalent SDOF system are also based on load and mass transformation factors, which are calculated to cause conservation of energy between the equivalent SDOF system and the component assuming a deformed component shape and that the deflection of the equivalent SDOF system equals the maximum deflection of the component at each time. For flexural behavior of one way reinforced concrete slabs subject to blast loads, SBEDS uses the resistance deflection curve shown in figure 2-5 for SDOF analysis. The maximum deflection of the equivalent SDOF mass-system is determined by the solving the following equation 11.

$$K_M M_c u''(t) + K_L C_c u'(t) + K_L R_c(u(t)) = K_L F_c(t)$$

……Equation 11

Here,

K_M = Mass conversion factor

M_c = Mass of the slab

K_L = Load conversion factor

C_c = Damping coefficient of the slab

$R_c u(t)$ = Resistance of slab

$F_c(t)$ = Load history of the blast load on the slab

The Unified Facilities Criteria (UFC) 3-340-02(Polcyn and Myers 2010) presents methods of design for protective construction used in facilities for development, testing, production, storage, maintenance, modification, inspection, demilitarization, and disposal of explosive materials. The transformation factors, or the load factors, mass factors, and load-mass factors used in SBEDS are identical to those defined in UFC 3-340-02. Although SBEDS generally follows the same approach as discussed in UFC 3-340-02 and the calculation in SBEDS for the resistance and stiffness for 1-way components exactly matches the approach in UFC 3-340-02 only when pure flexural response is involved. There are differences in the SBEDS and UFC 3-340-02 methodologies when more than one response are involved. For reinforced concrete sections, the formulas in SBEDS to calculate the dynamic concrete and reinforcement strength are based on the approach in UFC 3-340-01, which differs from the approach in UFC 3-340-02. UFC 3-340-02 allows the dynamic material strengths to be increased for larger deflections to account for strain hardening that could take place. This increased strength is calculated with a weighted average of the

dynamic yield strength and the dynamic tensile strength. SBEDS does not have this type of procedure programmed. The input parameters used for SDOF analysis using SBEDS in this research study are presented in table 3-3. Typical input data sheet for SBEDS analysis of the slab with ρ=0.46% is shown in figure B-1 of Appendix B.

Table 3-3: Input variables in SBEDS

Description	**Input Value**
Density of Concrete	150 pcf
Compressive strength of Concrete	4000 psi
Poisson's Ratio	0.18
Yield Strength of Reinforcement	60000 psi
Static Increase Factor (SIF)	1.1
Dynamic Increase factor (DIF)	1.19
Type of Cross Section	Type I

3.5. Slab Models and Geometry

This section describes the slab models, boundary conditions, the nature of blast loading, the material models used in LSDYNA, the types of analyses run, the damage criterion and the output variables studied.

The slab model is 64 inches in span, 34 inches in width and 4 inches in depth. The slab is modeled and meshed using eight-node hexahedral constant stress solid elements. The size of a solid element is 1 inch cube. The longitudinal and transverse reinforcement are modeled as beam element with truss formulation. The center line of the reinforcement bars is modeled at 1 inch from the bottom surface of concrete slab. Each beam element is 1 inch in length and modeled with different node numbers than the solid element nodes at the same location. The concrete and reinforcement elements are connected through Lagrange

constraints, which is equivalent to a master slave nodal relationship in conventional finite element modeling. These element sizes results in a model that consists of 11,851 nodes, 8,704 solid elements and 490 beam elements for 8 inch spacing of longitudinal reinforcement. For 4 inch spacing of longitudinal reinforcement, there are 12117 nodes, 8,704 solid elements and 780 beam elements. #3 reinforcement bars at 12 inch spacing are used as transverse reinforcement for all the four slabs. However, the longitudinal reinforcement is varied as follows:

a) **Slab 1:** #3 reinforcement bars at 8 inch spacing
b) **Slab 2:** #4 reinforcement bars at 8 inch spacing
c) **Slab 3:** #3 reinforcement bars at 4 inch spacing
d) **Slab 4:** #4 reinforcement bars at 4 inch spacing

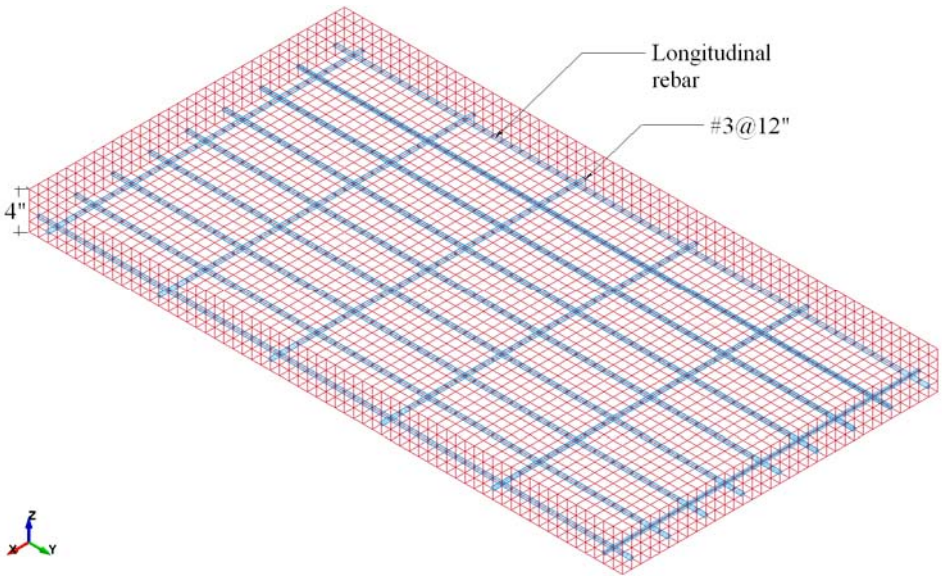

Figure 3-2: Isometric view of the slab model in LS DYNA

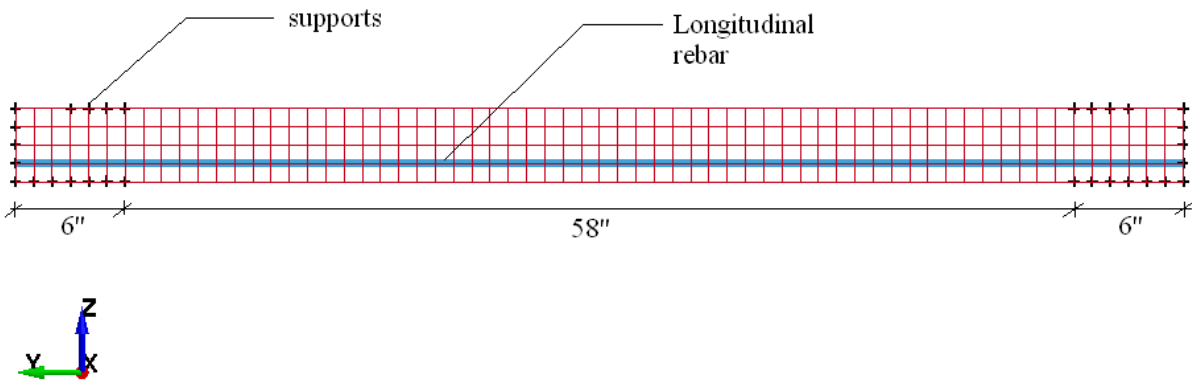

Figure 3-3: Longitudinal view of the slab model in LS DYNA

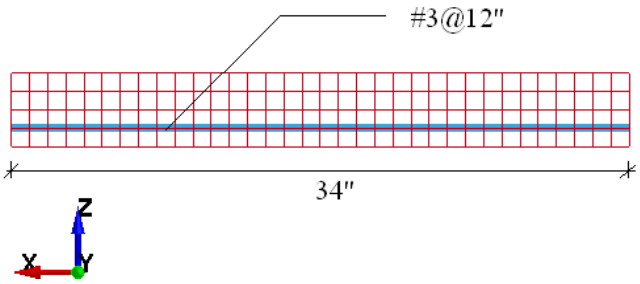

Figure 3-4: Transverse view of the slab model in LS DYNA

The reinforcement ratios of the four slabs are as indicated in table 3-4. The slab panel is supported at both ends using a steel frame, which restricts the translational displacement of the slab at supports. The length of the support is 6 inches on each end at the bottom face and hence the effective span is considered as 58 inches between centerline of supports. The nodes of concrete solid elements at the support locations are restricted against translation as shown in figure 3-3 to simulate the actual test conditions.

Table 3-4: Slab reinforcement details

Slab Description	Transverse	Longitudinal	Longitudinal
Slab 1	#3 @ 12“	#3 @ 8“	0.46%
Slab 2	#3 @ 12“	#4 @ 8“	0.82%
Slab 3	#3 @ 12“	#3 @ 4“	0.92%
Slab 4	#3 @ 12“	#4 @ 4“	1.64%

3.5.1. Slab Types

The selection of the slab properties including, geometry, thickness, material strength, restraint locations and type was based upon available 1/3 scale experimental models. The four slabs considered represent four different reinforcement ratios and two rebar spacing. The reinforcement ratio varies from 0.46% to 1.64%. This covers the range of reinforcement ratios normally used in design of reinforced concrete slabs for ductile behavior. The crack propagation and ductility of reinforced concrete slabs is affected by rebar spacing. Hence two longitudinal rebar spacing; 4" and 8" are considered in this study. The transverse reinforcement is spaced at 12" consistent with the experimental slabs. Normal reinforced concrete and normal strength reinforcement are considered for the four slab types. The primary objective of this research was to study and compare different analysis approaches in estimating the blast response of reinforced concrete slabs. The above considered variations provide the tools to achieve the above objective.

3.5.2. Modeling of Slab in LSDYNA and SBEDS

The selection of mesh size and material models was based upon results observed in parallel research. Mesh size of 1 inch was used as it was observed during other studies to give reasonably accurate results. The efficiency of Winfrith Concrete model for modeling concrete and Plastic Kinematic model for reinforcement is well documented in current research. Hence these superior material models are used in conjunction with the master-slave relationship between the concrete and reinforcement elements. The type of blast loading used in LS-DYNA can greatly impact the results. The load time history method and triangular idealization of load time history are validated in several research studies and

hence are used in this study. The pressures generated from the triangular load application were also validated with SBEDS and several other commonly used tools like AT BLAST. The slab was analyzed as a two-way 3-D model in LS-DYNA as compared to a one-way slab in SBEDS.

3.6. Natural Time Period and Frequency

The fundamental period for an elastic slab with pinned supports and subjected to a uniformly distributed force is computed as follows. With a modulus of elasticity of concrete of 3,605 *ksi* (compressive strength of concrete of 4 *ksi)* and assuming that the effective moment of inertia of the slab to be 25 percent of its gross moment of inertia as per ACI 318-08, $I_{eff} = 0.25 \times \frac{1}{12} \times 3^3 \times 12 = 6.75 \text{in}^4$. The maximum deflection is given by the equation $\Delta_{\max} = \frac{wl^4}{384 E_c I_{eff}} = \frac{(1k/in)(58in)^4}{384 \times 3,605ksi \times 6.75in^4} = 1.21in$ from which the stiffness is calculated as follows

$$K = \frac{1\ k/in\ \times 58in}{\Delta_{\max}\ in} = \frac{1\ k/in\ \times 58in}{1.21\ in} = 47.93 k/in$$

The mass of the slab is $m = 150/(12^3 \times 386.4) lb/in^3 \times 1 \times 4 \times 64 in^3 / 1000 = 5.7 \times 10^{-5} kips\, sec^2/in$ from which the fundamental period is calculated as

$$T_n = 2\pi\sqrt{\frac{m}{K}} = 2\pi\sqrt{\frac{5.7 \times 10^{-5}}{47.93}} = 0.0068s = 6.8ms$$

3.7. Blast Loading

LS-DYNA provides different ways to apply the pressure from a blast load to a structure. The blast load can be generated by using the Load_Blast_Enhanced command of LS-DYNA or by specifying a load curve and directly applying the pressure load. It is

required to specify the standoff distance and charge weight while using the Load_Blast_Enhanced option. The Load_Blast_Enhanced option also enables the researcher to record the pressure history calculated and applied by the LS-DYNA software internally. The peak pressures observed by using Load_Blast_Enhanced command were not correlating with other conventional software SBEDS, AT BLAST. Hence a triangular pressure load was directly applied in this research.

3.8. Pressure Impulse Curves for RC Slab

Development of PI curves is an iterative and time consuming process. Since SBEDS is developed based upon simplified approach, the program iteratively determines pressure impulse curves for reinforced concrete slabs. These pressure impulse regions from SBEDS were used as a starting point to start generating pressure impulse curves in LS-DYNA. Each data point in these pressure impulse curves represents an individual analysis. The pressure impulse curves were generated for the four slabs and three damage levels using SBEDS and LS-DYNA.

3.8.1. Development of PI Curves using SBEDS

Development of PI curves using SBEDS is an iterative process which is computed internally in the program. However, the slab details and basic parameters of blast analysis as discussed in previous sections need to input into the SBEDS program for initial SDOF analysis. Once the initial analysis is performed, the user can set up the damage levels for which PI curves are required. SBEDS program uses extensive iterative process by running multiple iterations of SDOF analysis for each data point required in each PI curve. All this analysis is performed internally and the PI curves are given as output as graphs and tables.

The PI curve data generated by the SBEDS program for the slab with 0.92% reinforcement is shown in table 3-5.

Table 3-5: SBEDS PI curve data for RC slab with 0.92% reinforcement ratio

Point	**P-I Curve 1**		**P-I Curve 2**		**P-I Curve 3**	
Number	Max. Defl.=1.17 in		Max. Defl.=2.33 in		Max. Defl.=3.5 in	
	Impulse (psi-ms)	Pressure (psi)	Impulse (psi-ms)	Pressure (psi)	Impulse (psi-ms)	Pressure (psi)
1	240.8	592.3	355.5	874.4	441.1	1085.1
2	242.7	298.5	354.5	436.0	436.2	536.5
3	244.4	150.3	354.1	217.8	433.7	266.7
4	251.0	102.9	361.3	148.1	440.4	180.5
5	263.4	81.0	370.7	114.0	449.1	138.1
6	278.5	68.5	385.8	94.9	464.1	114.2
7	322.0	52.8	427.3	70.1	507.8	83.3
8	380.1	46.7	484.7	59.6	559.1	68.8
9	615.1	37.8	737.1	45.3	811.3	49.9
10	864.2	35.4	1001.6	41.1	1081.4	44.3
11	1357.0	33.4	1533.9	37.7	1628.0	40.0
12	2603.4	32.0	2871.9	35.3	2996.7	36.9
13	5090.5	31.3	5538.9	34.1	5717.8	35.2
14	7578.5	31.1	8182.3	33.5	8418.6	34.5
15	15033.3	30.8	16149.0	33.1	16622.2	34.1

3.8.2. Development of PI Curves using LS DYNA

PI curves are not developed internally in LS-DYNA. Each simulation in LS-DYNA represents one load combination of pressure and impulse and the deflection is given as an output of the simulation. PI curve for any chosen damage level (deflection) represents a set of pressure and impulse values that give the same damage level. Hence it is evident that several analysis simulations are required in LS-DYNA to determine each single data point on the PI curve for each damage level. The PI curve data generated by SBEDS was used as a guideline and several simulations were performed in LS-DYNA iteratively to determine the

PI curves. The 2% damage level PI curve data generated using LS-DYNA for slab with 0.46% is shown in table 3-6.

Table 3-6: LS DYNA 2% damage level PI curve data for RC slab with 0.92% reinforcement ratio

Point Number	Impulse	Pressure	Time Duration	Maximum Deflection	Damage %
	psi-ms	psi	sec	in	%
1	132	500	0.000528	1.14	1.97
2	126	250	0.001008	1.12	1.93
3	123	131	0.001878	1.16	2.00
4	117	58	0.004034	1.2	2.07
5	128	24	0.010667	1.18	2.04
6	157	16	0.019625	1.26	2.17
7	196	12	0.032667	1.21	2.09
8	300	10	0.06	1.19	2.05
9	500	9.1	0.10989	1.21	2.09
10	1000	8.30	0.240964	1.18	2.04
11	2500	8.2	0.609756	1.26	2.17
12	5000	7.8	1.282051	1.21	2.09
13	10000	7.8	2.564103	1.24	2.14
14	20000	7.8	5.128205	1.2	2.07

3.8.3. PI Curves for the Four Slabs

Pressure impulse curves were developed for each of the four slabs using SBEDS and LS-DYNA. Slab 1 has the lowest longitudinal reinforcement ratio at 0.46% and Slab 4 has the highest longitudinal reinforcement ratio at 1.64%. Slabs 2 and 3 have similar reinforcement ratios but slab 2 has two times the rebar spacing as slab 3. Figures 3-5, 3-6, 3-7 and 3-8 show the PI diagrams for slabs 1, 2, 3 and 4 respectively. The dashed lines represent the PI diagrams generated by the SDOF analysis using SBEDS in which the diagrams were generated to represent 2%, 4% and 6% damage per the criterion used in this research. The three levels of damage correspond to a peak central deflection of 1.17 in, 2.33

in and 3.50 in respectively. The second set of PI curves shown, represented by solid lines, is the curves generated using LSDYNA simulations. The symbols for each damage level are identical, with the triangles, circles and squares representing 2%, 4% and 6% damage levels respectively.

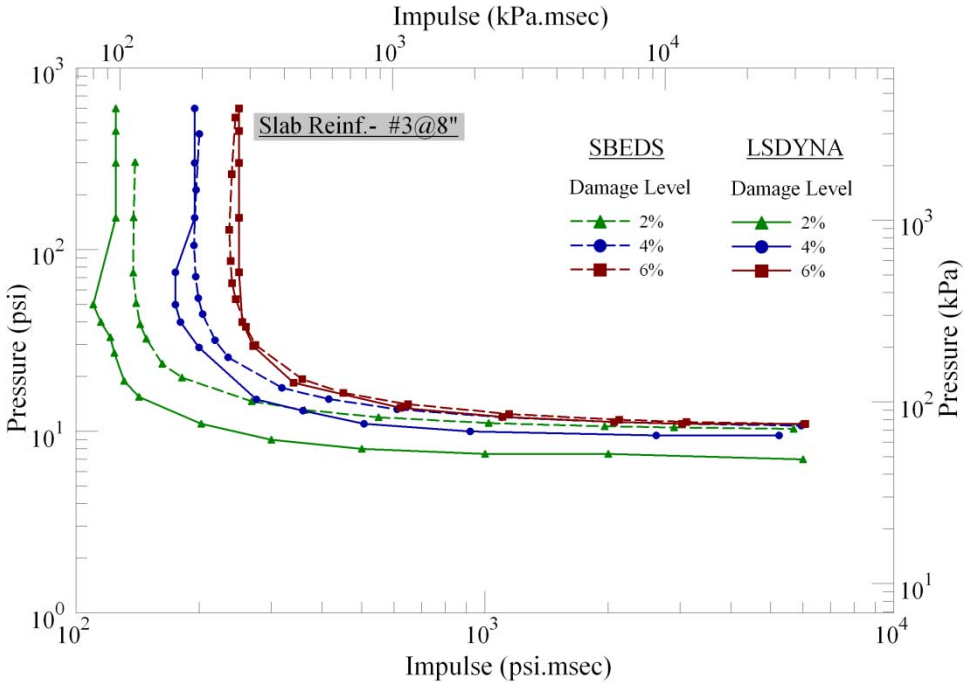

Figure 3-5: Pressure-Impulse Curves for Slab with ρ = 0.46%

Table 3-7: Typical Pressure Impulse Values for Slab with ρ =0.46%

Damage Level	Analysis Procedure	Pressure	Impulse	Pressure	Impulse	Pressure	Impulse
		psi	psi-ms	psi	psi-ms	psi	psi-ms
		Impulse Regime		Dynamic Regime		Quasi-Static Regime	
2% damage	SBEDS	303	139	20	181	10	5690
	LSDYNA	300	125	16	142	7	6000
4% damage	SBEDS	435	200	26	235	11	5929
	LSDYNA	450	195	29	200	10	5239
6% damage	SBEDS	534	245	30	275	11	6034
	LSDYNA	600	250	30	271	11	6067

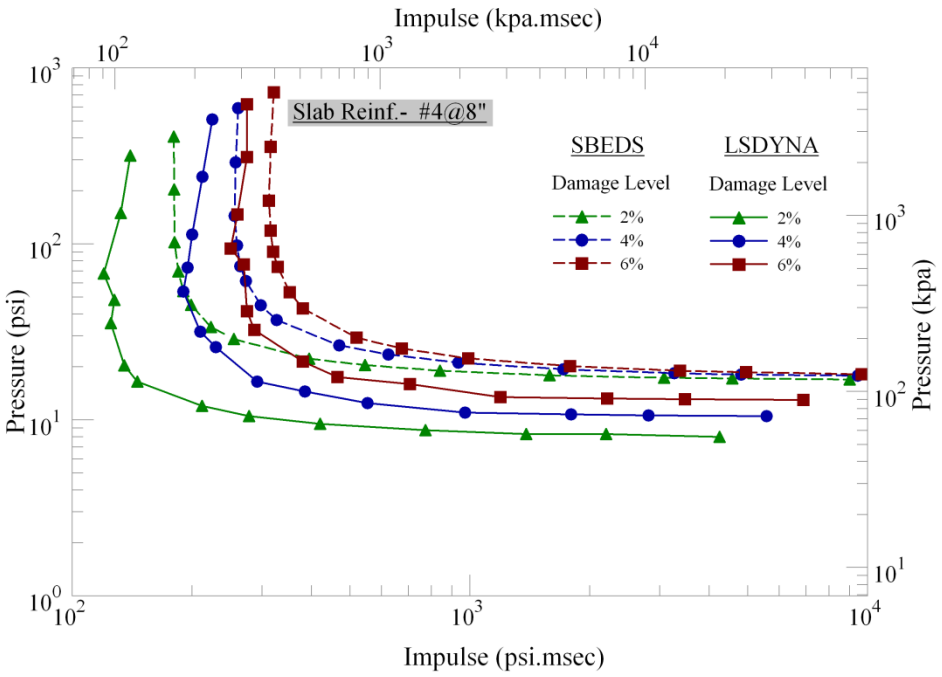

Figure 3-6: Pressure-Impulse Curves for Slab with ρ = 0.82%

Table 3-8: Typical Pressure Impulse Values for Slab with ρ =0.82%

Damage Level	Analysis Procedure	Pressure	Impulse	Pressure	Impulse	Pressure	Impulse
		psi	psi-ms	psi	psi-ms	psi	psi-ms
		Impulse Regime		Dynamic Regime		Quasi-Static Regime	
2% damage	SBEDS	408	180	29	255	17	4566
	LSDYNA	317	140	17	146	8	4241
4% damage	SBEDS	591	261	37	326	18	4803
	LSDYNA	510	225	26	230	11	5566
6% damage	SBEDS	727	321	43	380	19	4948
	LSDYNA	623	275	33	287	13	6891

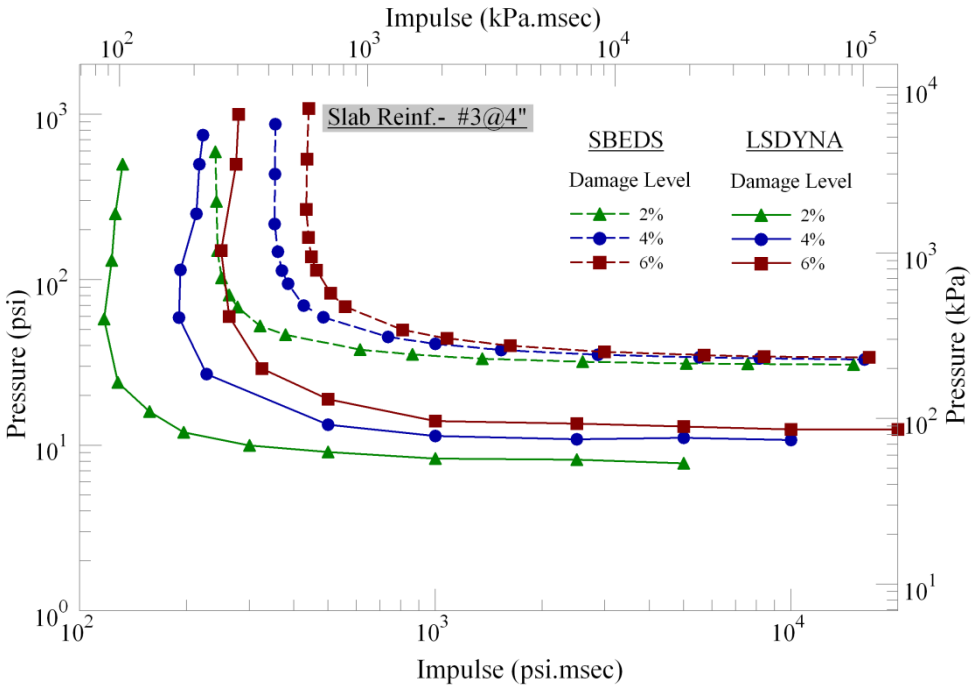

Figure 3-7: Pressure-Impulse Curves for Slab with ρ = 0.92%

Table 3-9: Typical Pressure Impulse Values for Slab with ρ =0.92%

Damage Level	Analysis Procedure	Pressure	Impulse	Pressure	Impulse	Pressure	Impulse
		psi	psi-ms	psi	psi-ms	psi	psi-ms
		Impulse Regime		Dynamic Regime		Quasi-Static Regime	
2% damage	SBEDS	591	241	47	380	31	5082
	LSDYNA	500	132	16	157	8	5000
4% damage	SBEDS	873	355	59	484	33	8168
	LSDYNA	750	222	27	228	11	10000
6% damage	SBEDS	1083	441	69	558	34	16592
	LSDYNA	1000	280	29	325	13	20000

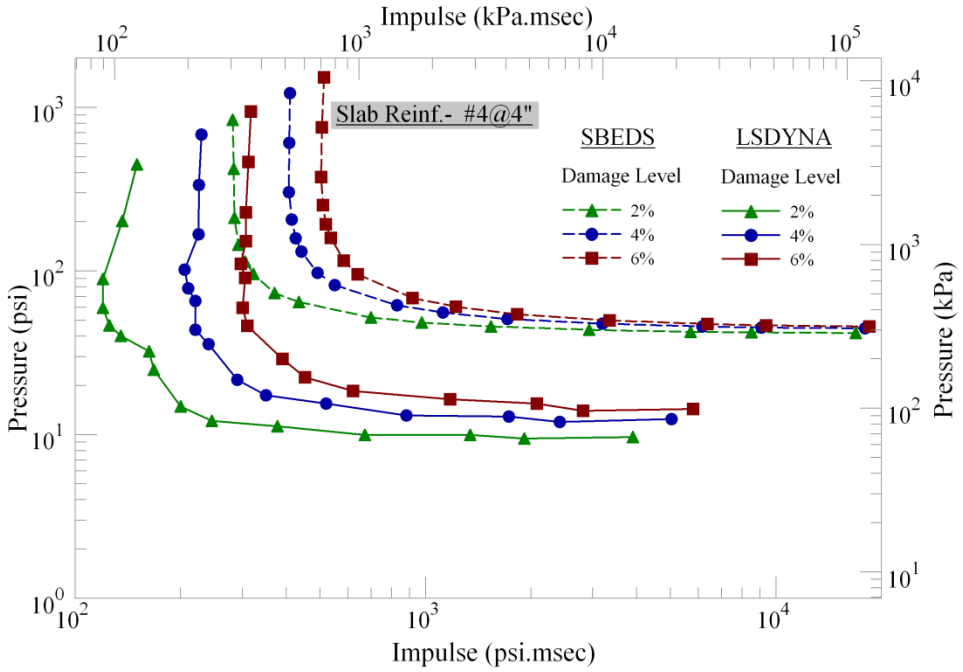

Figure 3-8: Pressure-Impulse Curves for Slab with ρ = 1.64%

Table 3-10: Typical Pressure Impulse Values for Slab with ρ =1.64%

Damage Level	Analysis Procedure	Pressure	Impulse	Pressure	Impulse	Pressure	Impulse
		psi	psi-ms	psi	psi-ms	psi	psi-ms
		Impulse Regime		Dynamic Regime		Quasi-Static Regime	
2% damage	SBEDS	423	283	65	435	43	5702
	LSDYNA	448	150	25	168	10	3901
4% damage	SBEDS	609	408	82	550	46	6156
	LSDYNA	684	229	22	290	13	5027
6% damage	SBEDS	755	506	95	640	48	6374
	LSDYNA	946	317	46	310	14	5791

3.8.4. PI Curves for the Three Damage Levels

Pressure impulse curves developed using SBEDS and LS-DYNA for the four slabs was also compared for each damage level considered. Three different damage levels were

considered in this study. The three damage levels considered, 2%, 4% and 6% correspond to peak central deflection of 1.17 in, 2.33 in and 3.50 in respectively. Figures 3-9, 3-10 and 3-11 show the PI diagrams for damage levels 2%, 4% and 6% respectively for all slabs. The symbols for each slab are identical, with the triangles, circles, squares and diamonds representing slabs 1, 2, 3 and 4 respectively. The dashed lines represent the PI diagrams generated by the SDOF analysis using SBEDS and the second set of PI curves shown, represented by solid lines, is the curves generated using LSDYNA simulations.

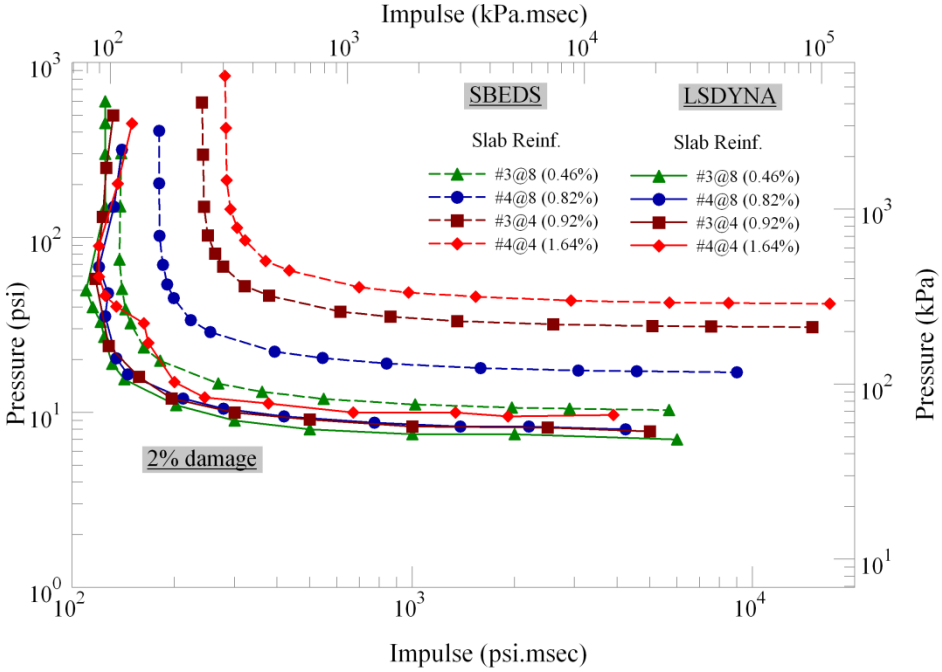

Figure 3-9: Pressure-Impulse Curves for 2% Damage Level

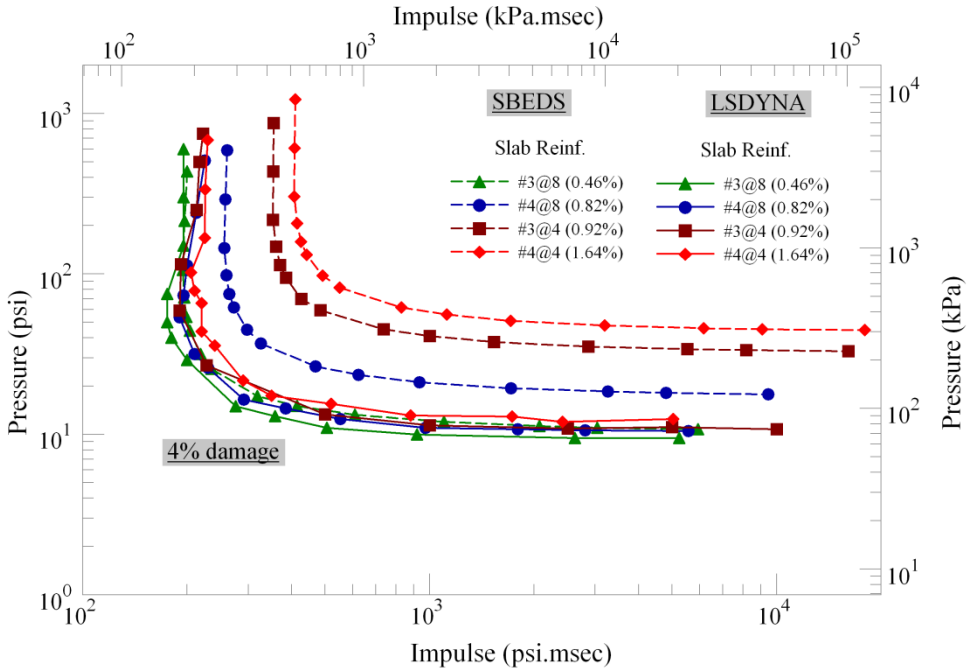

Figure 3-10: Pressure-Impulse Curves for 4% Damage Level

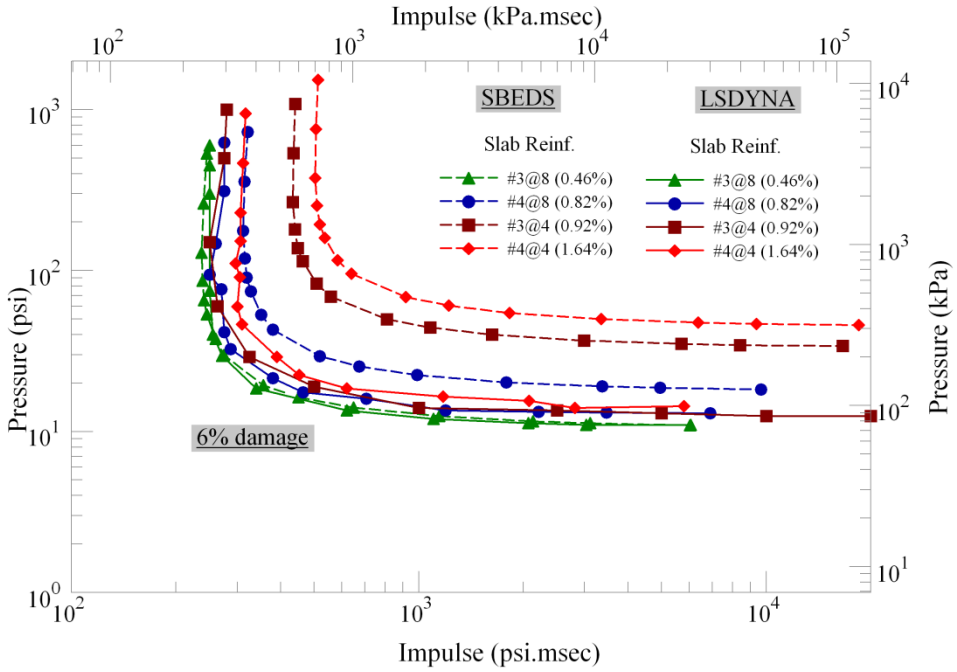

Figure 3-11: Pressure-Impulse Curves for 6% Damage Level

3.9. Curve Fit Analysis for LSDYNA PI Curves

A curve fit analysis was carried out considering the independent variables to be the longitudinal reinforcement ratio, damage level and load duration in order to predict the pressure values. The resulting equation is expressed as shown in equation 12

$$\log(p_r) = A + B \times \Delta + C \times Col + D \times \log(t_d) + E \times \log(t_d^2) + F \times \log(t_d^3) + G \times \log(t_d^4) + H \times \log(t_d^5)$$

……Equation 12

Where *A*, *B*, *C*, *D*, *E, F, G and H* are coefficients outlined in Table 3-7. In the equation Δ represents the damage level and can take values of 2, 4 and 6, Col represents reinforcement ratio and t_d represents the load duration in milliseconds.

Table 3-11: Coefficients developed for PI curves for the four slabs

A	B	C	D	E	F	G	H
0.677212	0.073588	0.067693	-0.03089	-0.10111	-0.12806	0.003796	0.005588

Figures 3-12, 3-13, 3-14 and 3-15 compare the LS DYNA PI curves for slabs 1, 2, 3 and 4 respectively with those developed from the curve fit equation. The dashed lines represent the PI diagrams generated by the curve fit equation. The second set of PI curves shown, represented by solid lines, is the curves generated using LSDYNA simulations. The symbols for each damage level are identical, with the triangles, circles and squares representing 2%, 4% and 6% damage levels respectively. The equation developed characterize the blast pressure and time duration that can be used in deriving pressure impulse (PI) curves for the four slabs used in this research study. This can be used as a convenient tool to interpolate PI curves for different reinforcement ratio and damage levels other than 2%, 4% and 6% used for developing PI curves in this research study.

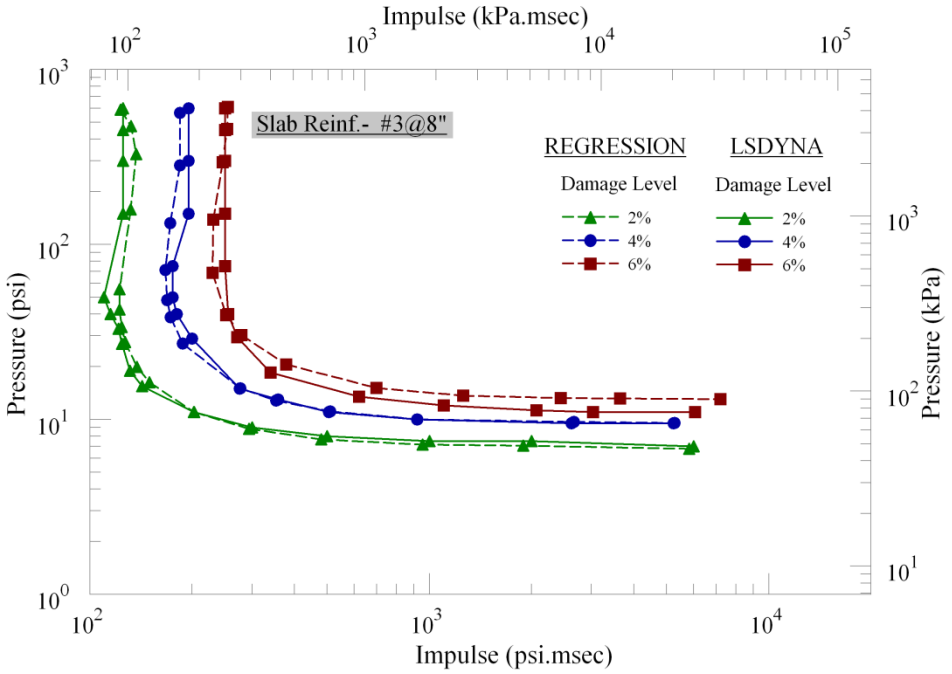

Figure 3-12: Pressure-Impulse Curves using Curve Fit Analysis for Slab with ρ = 0.46%

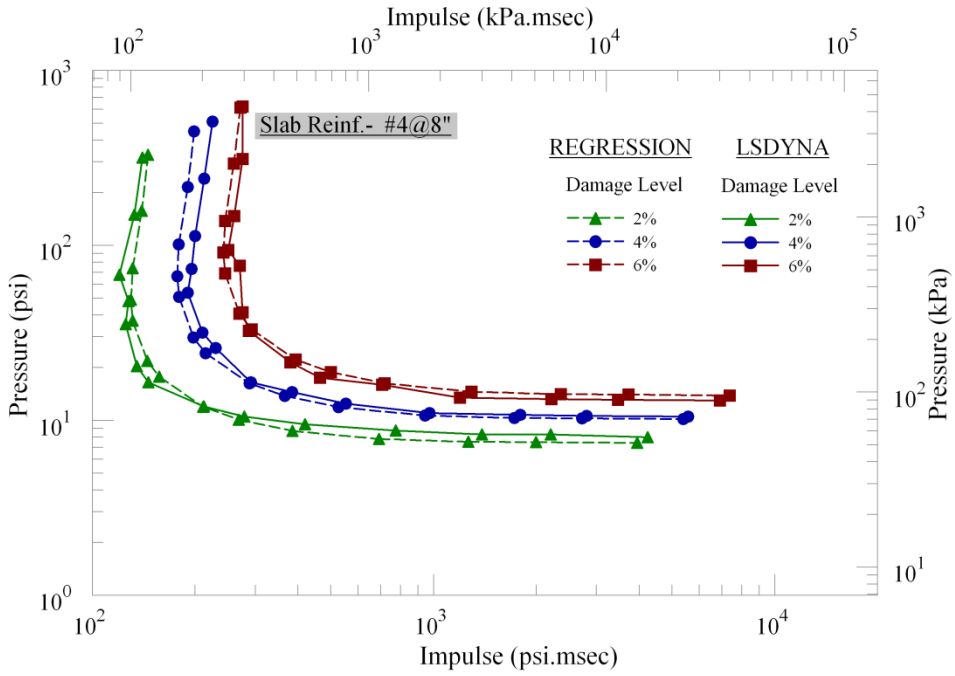

Figure 3-13: Pressure-Impulse Curves using Curve Fit Analysis for Slab with ρ = 0.82%

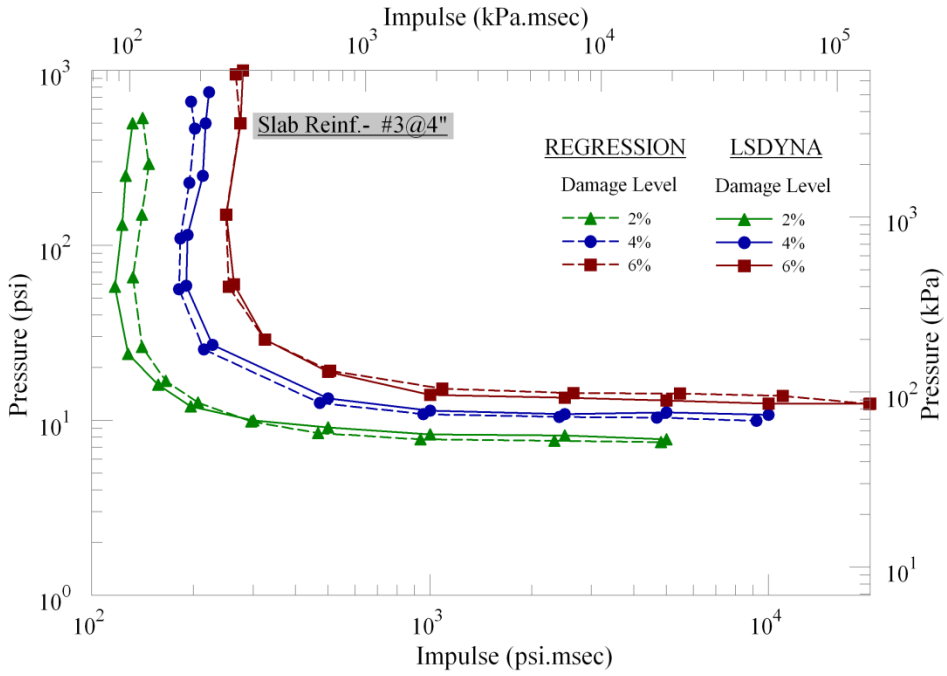

Figure 3-14: Pressure-Impulse Curves using Curve Fit Analysis for Slab with ρ = 0.92%

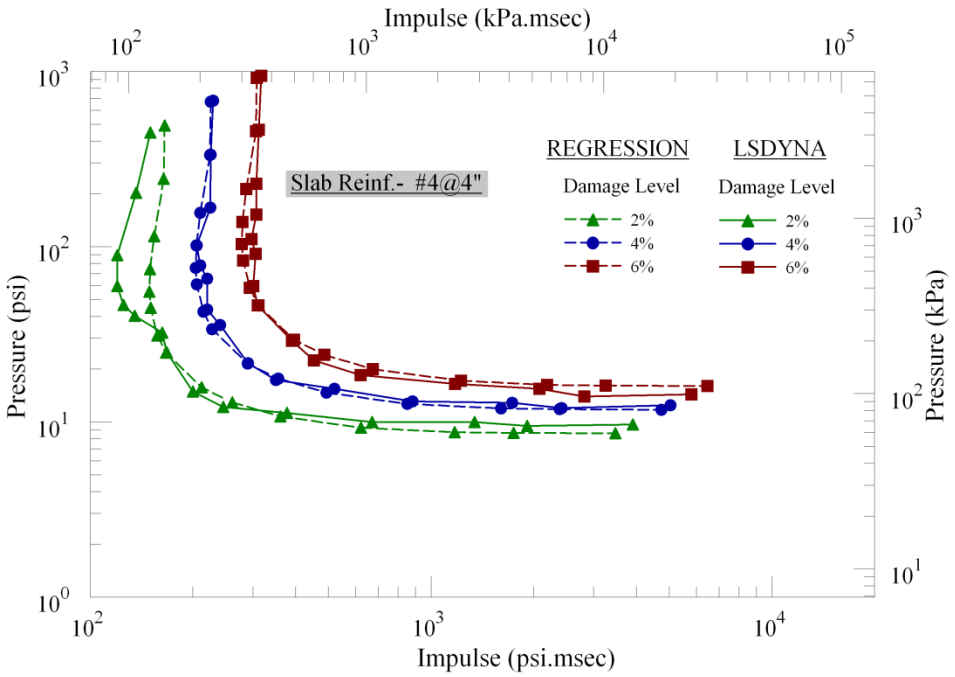

Figure 3-15: Pressure-Impulse Curves using Curve Fit Analysis for Slab with ρ = 1.64%

3.10. Displacement Contours for the Three Loading Regimes

Figures 3-16 to 3-18 show the deflected shapes from the finite element simulation of the RC slab with ρ = 0.46% and damage level = 6% for the three loading regimes. It can be seen that the flexural mode of failure is predominant in all the three cases. However, the deflected shapes correspond to both flexural and shear deformation of the RC slab. The deviatoric strains in the concrete model correspond to the shear deformation of the RC slab. Figure 3-19 and figure 3-20 show the infinitesimal shear strain and maximum principal strain of the RC slab with ρ = 0.46% and damage level = 6% in the dynamic loading regime. It can be seen from figures 3-19 and 3-20 that shear deformation can have a major contribution to the total deformation even for flexural mode of failure observed in the deflected shapes of the RC slab shown in figures 3-16 to 3-18. Similar deflection patterns were observed for all the slabs and all damage levels.

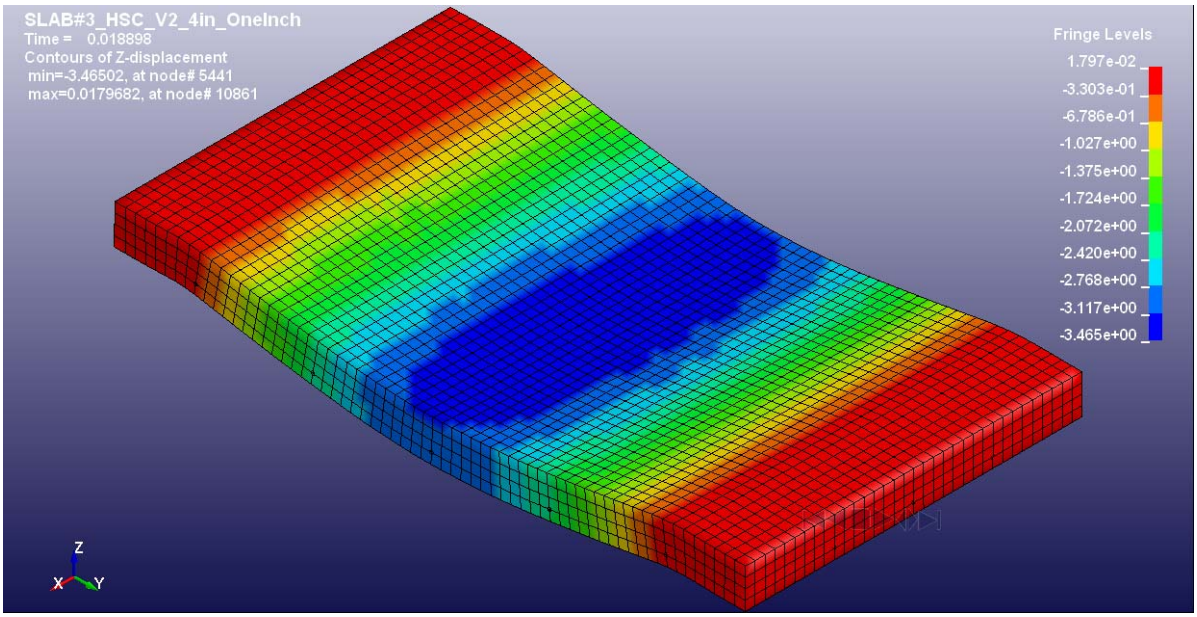

Figure 3-16: Displacement Contour of RC Slab with ρ = 0.46% and Damage Level = 6% in Impulse Loading Region

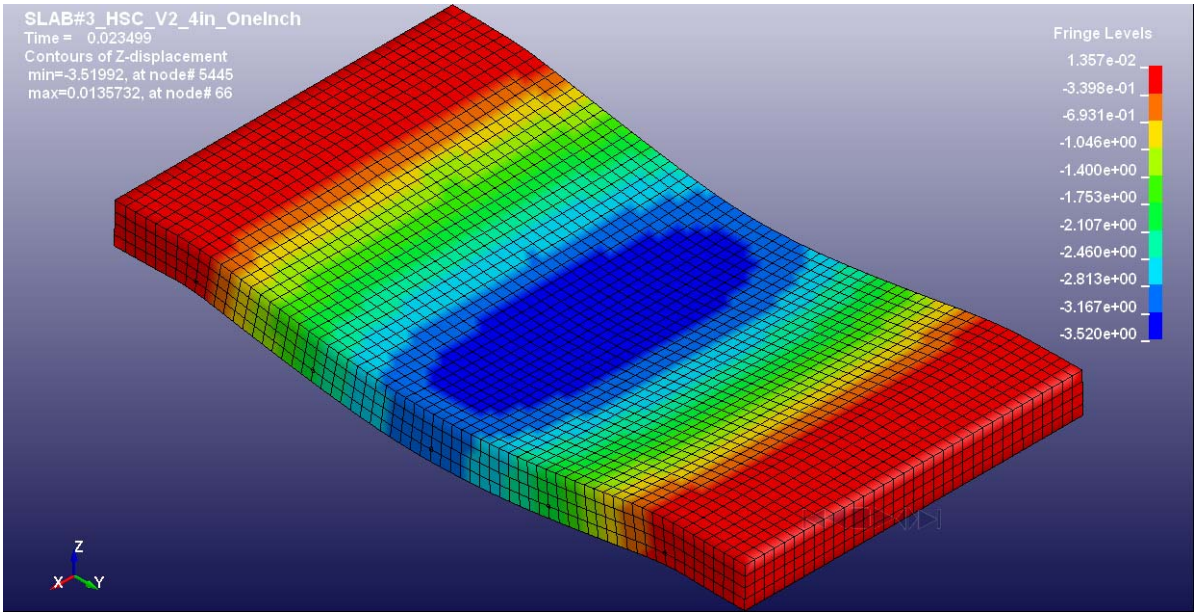

Figure 3-17: Displacement Contour of RC Slab with ρ = 0.46% and Damage Level = 6% in Dynamic Loading Region

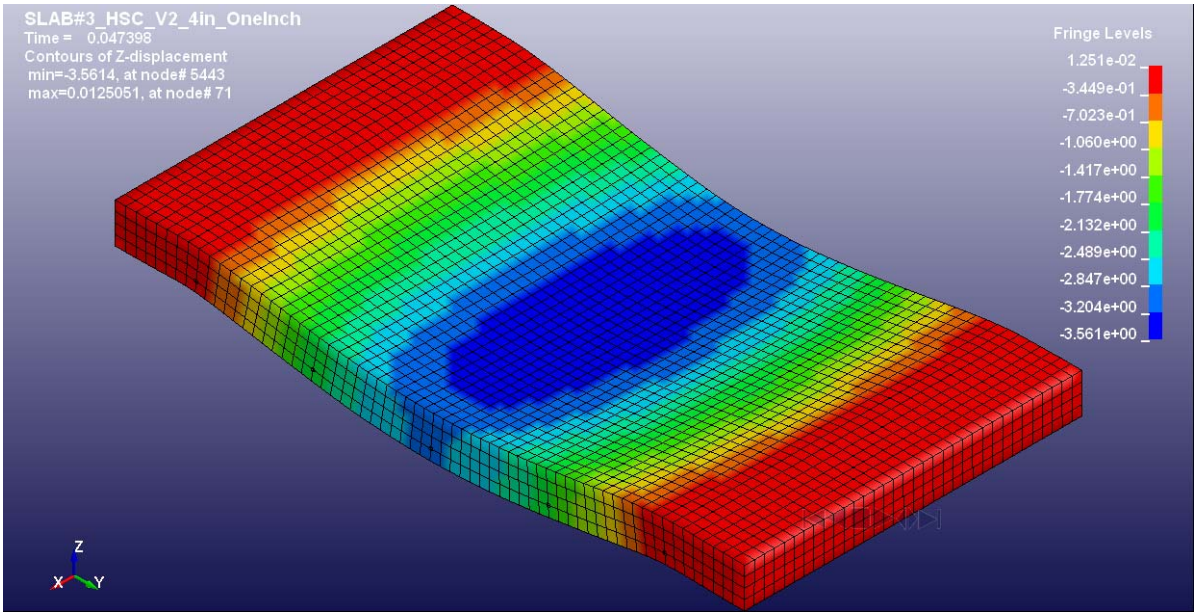

Figure 3-18: Displacement Contour of RC Slab with ρ = 0.46% and Damage Level = 6% in Quasi-Static Loading Region

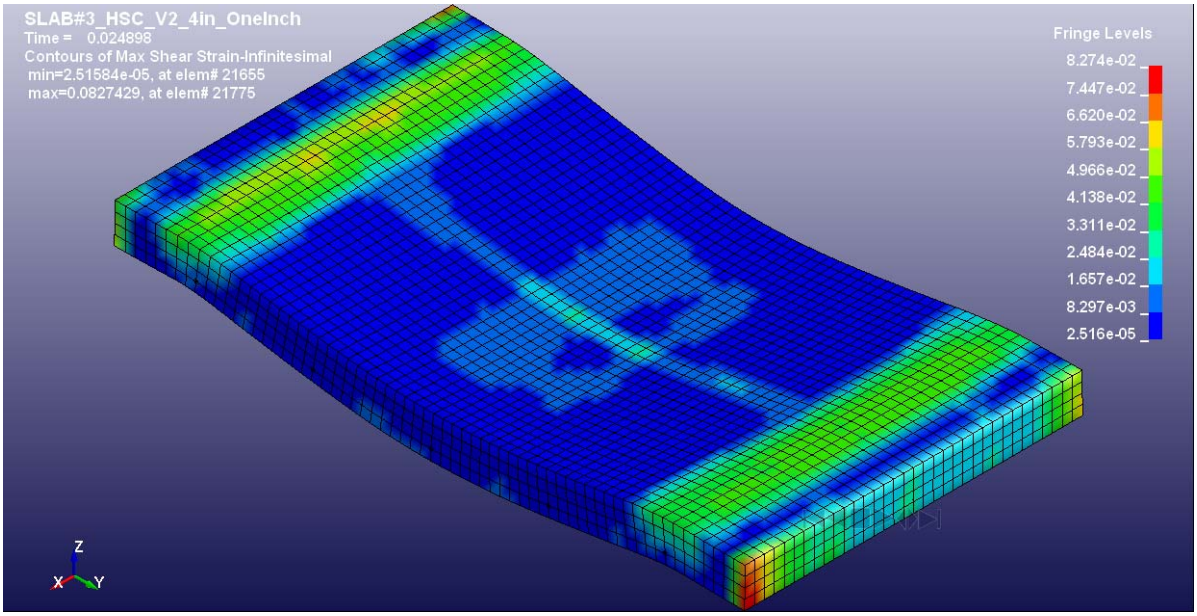

Figure 3-19: Infinitesimal Maximum Shear Strain for RC Slab with ρ = 0.46% and Damage Level = 6% in Dynamic Loading Regime

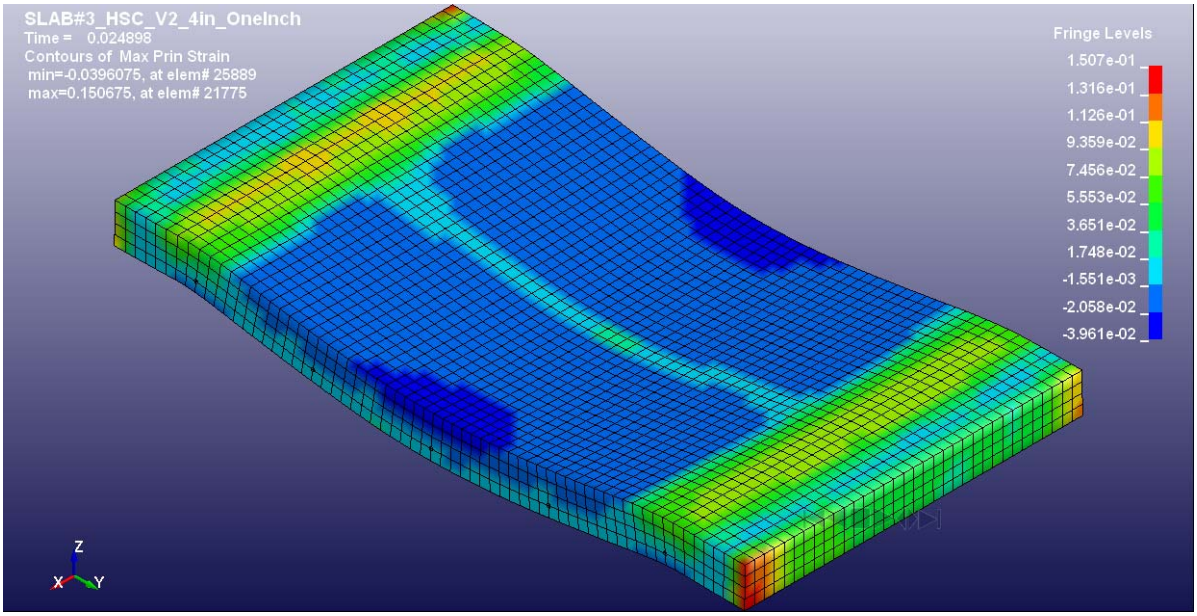

Figure 3-20: Maximum Principal Shear Strain for RC Slab with ρ = 0.46% and Damage Level = 6% in Dynamic Loading Regime

3.11. Discussion of Results

This research is an attempt to understanding the response of reinforced concrete slabs subjected to blast and impact loading. The effect of various parameters on the blast performance of reinforced concrete slabs is also discussed below.

3.11.1. PI Curves for RC Slab with 0.46% Reinforcement Ratio

It can be observed from figure 3-5 that the PI curve for 2% damage level developed using LS-DYNA is conservative as compared to the corresponding PI curve developed using SBEDS. However, this difference is reduced as the damage level is increased from 2% to 6%, and the PI curve for 6% damage level using SBEDS and LS-DYNA closely match each other. The difference in the PI curves developed using SBEDS and LS-DYNA is more in the dynamic loading region as compared to impulse and quasi-static loading region for 2% and 4% damage levels.

3.11.2. PI Curves for RC Slab with 0.82% Reinforcement Ratio

It can be observed from figure 3-6 that the PI curve for all three damage levels developed using LS-DYNA is conservative as compared to the corresponding PI curves developed using SBEDS. However, this difference is marginally reduced as the damage level is increased from 2% to 6%. The difference in the PI curves developed using SBEDS and LS-DYNA is more in the dynamic loading region as compared to impulse and quasi-static loading region for all damage levels.

3.11.3. PI Curves for RC Slab with 0.92% Reinforcement Ratio

It can be observed from figure 3-7 that the PI curve for all three damage levels developed using LS-DYNA is conservative as compared to the corresponding PI curves developed using SBEDS. However, this difference is marginally reduced as the damage level is increased from 2% to 6%. The difference in the PI curves developed using SBEDS and LS-DYNA is more in the dynamic loading region as compared to impulse and quasi-static loading region for 4% and 6% damage levels.

3.11.4. PI Curves for RC Slab with 1.64% Reinforcement Ratio

It can be observed from figure 3-8 that the PI curve for all three damage levels developed using LS-DYNA is conservative as compared to the corresponding PI curves developed using SBEDS. However, this difference is marginally reduced as the damage level is increased from 2% to 6%. The difference in the PI curves developed using SBEDS and LS-DYNA is only marginally greater in the dynamic loading region as compared to impulse and quasi-static loading region for all damage levels.

3.11.5. PI Curves for RC Slabs with 2% Damage Level

It can be observed from figure 3-9 that the PI curve for all four slabs developed using LS-DYNA is conservative as compared to the corresponding PI curves developed using SBEDS. However, this difference is increased as the reinforcement ratio is increased from 0.46% to 1.64%. The difference in the 2% damage level PI curves developed using SBEDS and LS-DYNA is considerably greater for the RC slab with #3@4” (0.92% reinforcement ratio) as compared to #4@8” (0.82% reinforcement ratio) even though the reinforcement

ratio is almost same. The variation with respect to loading regimes is discussed in previous sections.

3.11.6. PI Curves for RC Slabs with 4% Damage Level

It can be observed from figure 3-10 that the PI curve for all four slabs developed using LS-DYNA is conservative as compared to the corresponding PI curves developed using SBEDS. However, this difference is increased as the reinforcement ratio is increased from 0.46% to 1.64%, the PI curve for 0.46% reinforcement ratio using SBEDS and LS-DYNA closely match each other. The difference in the 4% damage level PI curves developed using SBEDS and LS-DYNA is considerably greater for the RC slab with #3@4" (0.92% reinforcement ratio) as compared to #4@8" (0.82% reinforcement ratio) even though the reinforcement ratio is almost same. The variation with respect to loading regimes is discussed in previous sections.

3.11.7. PI Curves for RC Slabs with 6% Damage Level

It can be observed from figure 3-11 that the PI curve for all four slabs developed using LS-DYNA is conservative as compared to the corresponding PI curves developed using SBEDS. However, this difference is increased as the reinforcement ratio is increased from 0.46% to 1.64%, the PI curve for 0.46% reinforcement ratio using SBEDS and LS-DYNA closely match each other. The difference in the 6% damage level PI curves developed using SBEDS and LS-DYNA is considerably greater for the RC slab with #3@4" (0.92% reinforcement ratio) as compared to #4@8" (0.82% reinforcement ratio) even

though the reinforcement ratio is almost same. The variation with respect to loading regimes is discussed in previous sections.

3.11.8. The Effect of Reinforcement Ratio

The reinforcement ratio in a reinforced concrete slab has a direct effect on ductility which is defined as the ability of the structure or structural element to undergo large amounts of deformation without complete failure. The pressure impulse curves developed from SBEDS clearly illustrated this phenomenon. As it can be observed from figures 3-5 to 3-9, the blast resistance of the reinforced concrete slab as illustrated by pressure impulse curves using SBEDS was improved by a good margin for each increment in reinforcement ratio. However, this effect was not as prominent in the pressure impulse curves using LS-DYNA. This can be attributed to the fact that the shear deflection keeps becoming more prominent and the flexural deflection keeps becoming lesser part of the total deflection as we keep increasing the ratio. As it can be observed from the figures 3-5 to 3-9, SBEDS and LS-DYNA showed a closer correlation in prediction of pressure impulse curves for Slab 1 which has 0.46% reinforcement. But as the reinforcement ratio was increased for other slabs, there was more disparity in the results. This could be attributed to the limited capability of SBEDS in modeling a more realistic shear response for dynamic loads.

3.11.9. The Effect of Reinforcement Spacing

The reinforcement spacing can have a significant affect in reducing the deflection by reducing the spacing due to improved effective moment of inertia of the concrete section. However this is more relevant for flexural deflection rather than shear deflection. Initial

observation of figures 3-6 and 3-7 for slabs 2 and 3 illustrate better compatibility of SBEDS and LS-DYNA generated pressure impulse curves.

3.11.10. The Effect of Damage Levels

Figures 3-9 to 3-11 illustrate that the two analysis approaches closely correlate at 2% damage level and the variation and discrepancy increases with increase in damage levels. As the damage level increases, the reinforced concrete slab elements transition from elastic behavior to inelastic behavior. Hence the observations in these figures can be attributed to the fact that LS-DYNA is advanced finite element software which accurately predicts non-linear response of reinforced concrete slabs.

CHAPTER 4

EXPERIMENTAL STUDY AND DESIGN VALUES

This chapter presents comparison of numerical results in previous chapter with experimental data and design examples. The current seismic detailing concepts and their applicability for blast resistance of reinforced concrete slabs are also discussed in this chapter.

4.1. Experimental Study

An experimental investigation on twelve 1/3 scale reinforced concrete slabs with single mat reinforcement. The experiments were performed by Dr. Ganesh Thiagarajan, Principal Investigator for this project, at the U.S. Army Engineering Research and Development Center, Vicksburg, MS. The primary objective of the experiment study was to compare use of High-strength concrete versus regular strength concrete in reinforced concrete slabs for resisting blast loads. The experiments were conducted in Blast Load Simulator (Shock Tube). Blast Load Simulator provides a controlled generation and uniform application of blast pressures on the face of the slab. The pressure versus time variation in both positive and negative phases can be accurately recorded in the blast load simulator.

The overall dimensions for the slab panels tested are 64 in. (1625 mm.) X 34in. (864 mm.) X 4 in. (101.6 mm.). Two material combinations based on strength were used in this study. The designation used for High-Strength material combination is “HSC-V” while the designation used for Normal-Strength materials is “RSC-R”. Concrete compressive strength of 4000 psi (27.58 Mpa) and Grade 60 conventional rebar with yield strength of 60000 psi (413.68 Mpa) was used for Normal-Strength materials. This numerical simulation in this

research thesis was based upon the slab geometry, boundary conditions of experimental slab panel with Normal-Strength materials “RSC-R”. The longitudinal rebar used was # 3 rebar at 4 inch and 8” spacing. The High-Strength material combination is not part of this thesis and hence not discussed here. The experimental program schedule with Normal-Strength materials is shown in table 4-1.

Table 4-1: Experimental program for Normal-Strength materials

Slab #	Slab Type	Date	Driver pressure	Explosion
Slab # 2	RSC - R1 - 4in.	12/14/2010	1150 psi	100% Air
Slab # 4	RSC - R2 - 4in.	12/16/2010	1150 psi	100% Air
Slab # 6	RSC - R3 - 4in.	02/01/2011	900 psi	100% Air
Slab # 8	RSC - R4 - 8in.	02/03/2011	700 psi	25% HE
Slab # 10	RSC - R5 - 8in.	02/07/2011	750 psi	25% HE
Slab # 12	RSC - R6 - 8in.	02/09/2011	725 psi	25% HE

The slab type denotation ‘RSC-RX-4in.’in table 4-1 corresponds to experimental slab panel with regular strength concrete and reinforcement with #3@4” spacing. And similarly, the slab type denotation ‘RSC-RX-8in.’corresponds to experimental slab panel with regular strength concrete and reinforcement with #3@8” spacing. Pressure data at six different locations on the slab was recorded in this experiment. The laser deflection measurement device and central accelerometers were used to record the deflection on the back face of the slabs. The average peak pressures and impulse with measured deflections for the six slabs with normal strength materials as reported with experimental data is reproduced here in table 4-2. The damage level is calculated as the percentage ratio of measured deflection tabulated below at the center to slab to the span of slab (58”).

Table 4-2: Experimental values for average pressure, impulse and measured deflections of various slabs

Slab Type	Slab Reinforcement	Average pressure	Average impulse	Measured deflection	Damage Level
		(psi)	(psi-msec)	(inches)	(%)
Slab#2	#3@4”	53	976	4.29	7.4%
Slab#4	#3@4”	53	1000	4.45	7.7%
Slab#6	#3@4”	45	785	3.17	5.5%
Slab#8	#3@8”	34	495	3.36	5.8%
Slab#10	#3@8”	35	550	3.6	6.2%
Slab#12	#3@8”	34	509	3.17	5.5%

The experimental study is not a part of this research thesis but the experimental data was compared with analytical results of SDOF and FE analysis performed in this research study for validation. The comparison is discussed in detail in later sections of this chapter.

4.2. Design of RC slab for Blast Loads

This section presents the design of reinforced concrete slab as per Unified Facilities Criteria UFC -340-02(Polcyn and Myers 2010). The Normal-Strength materials slab panel from experimental study with #3@4in. and #3@8in. longitudinal reinforcement are designed and results compared with experimental and numerical values. The pressure and impulse values for design of these slabs are iterated to achieve 3.17 inches of deflection as observed in experimental slabs#6 and #8 shown in table 4-2. The dynamic increase factors from table 4-1 of UFC 3-340-02 and the corresponding dynamic strength of materials are as below. The ductile mode of behavior is assumed to be in far design range developing a distribution of uniform blast load for this example.

Concrete:

Bending - 1.19

Diagonal tension - 1.00

Reinforcement:

Bending - 1.17

Diagonal tension - 1.00

Direct shear - 1.10

Concrete (f'_{dc}):

Compression - 1.19 (4,000) = 4,760 psi

Diagonal tension - 1.00 (4,000) = 4,000 psi

Reinforcement (f_{dv}):

Bending - 1.17 (60,000) = 70,200 psi

Diagonal tension - 1.00 (60,000) = 60,000 psi

Direct shear - 1.10 (60,000) = 66,000 psi

The slab types considered here are of Type I cross-section as defined in UFC 3-340-02. Type I cross section is as the reinforced concrete slab cross section where the concrete cover over the reinforcement on both surfaces of the element remains intact and the concrete is effective in resisting moment. Type II and Type III cross sections correspond to situations when Type I is not applicable i.e. the concrete is crushed or the concrete cover over reinforcement is completely disengaged.

4.2.1. Design of RC Slab with #3@4in. Longitudinal Rebar

The following steps are followed as recommended in UFC 3-340-02 for the design of the RC slab with #3@4in to achieve an inelastic deflection of 3.17 inches.

1. The minimum flexural reinforcement that needs to be provided as per table 4-3 of UFC 3-340-02 is $1.875\ \sqrt{f'_c}/f_y\ bd = 1.875\ \sqrt{4000} / 60000 \times 4 \times (2.81) = 0.02$ sq-in. Hence #3 rebar provided with $A_s = 0.11$ sq-in is okay.
2. The neutral axis depth $a = A_s f_{dv}/0.85bf'_{dc} = 0.11 \times 70200 / (0.85 \times 4 \times 4760) = 0.48$ inches. Hence the moment capacity $M_u = A_s f_{dv}/b \times (d-a/2) = 0.11 \times 70200/4 \times (2.81-0.48/2) = 4961$ lbs.-in / in.
3. Assuming the slab has one-way behavior with restraints not sufficient to prevent any rotation at ends, the ultimate resistance for unit width of slab, $r_u = 8(M_P)/L^2 = 8 \times (4961) / 58^2 = 11.8$psi.
4. Determination of modulus of elasticity and modular ratio:

   $$E_c = w^{1.5}\ 33\ (f'c)^{1/2} = (150)^{1.5}\ (33)(4000)^{1/2} = 3835 \times 10^3 \text{ psi}$$

   $$E_s = 29 \times 10^6 \text{ psi}$$

   $$n = E_s / E_c = 29 \times 10^6 / 3835 \times 10^3 = 7.5$$

5. Determination of average moment of inertia for an inch width of slab:

   $$I_g = 4^3/12 = 5.33 \text{ in}^4$$

   $I_c = Fd^3$. With modular ratio $n = 7.56$ and reinforcement ratio $\rho = A_s/bd = 0.11/(4 \times 3) = 0.0092$, $F = 0.043$ from figure 4-11 of UFC 3-340-02. Hence $I_c = 0.043 \times 2.81^3 = 0.954 \text{ in}^4$

   $$I_a = (I_g+I_c)/2 = 3.142 \text{ in}^4$$

6. Equivalent elastic stiffness and deflection:

$K_E = 384EI/5L^4 = 384x\ 3835x\ 10^3x\ 3.142 / (5x58^4) = 81.8$ psi / in.

The elastic deflection $X_E = r_u/K_E = 11.8 / 81.8 = 0.145$ inches.

7. Determination of natural time period:

   Mass, m = $(150/12^3)$ pci x 4 inch x 1 inch / (32*12) in /sec^2 x 10^6

   = 904 psi-msec^2/in

   $K_{LM} = (0.78+0.66)/2 = 0.72$

   $T_N = 2\ \pi\ \sqrt{}\ (m/K_E) = 2\ \pi\ \sqrt{}\ (0.72 \times 904 / 81.8) = 17.7$ msec

   Duration of load T = 2 x 785 / 45 = 34.9 msec

8. Determination of pressure and impulse values:

   For achieving 3.17 inches of maximum deflection observed in experiment, $X_M/X_E = 3.17 / .145 = 21.9$ and $T/T_N = 34.9 / 17.7 = 1.97$. From table 3-54, ru/P = 0.575, hence peak pressure P = 11.8 / 0.575 = 20.5 psi and corresponding impulse for a load duration of 34.9 msec = 0.5 x 34.9 x 20.5 = 358 psi-msec.

4.2.2. Design of RC Slab with #3@8in. Longitudinal Rebar

The following steps are followed as recommended in UFC 3-340-02 for the design of the RC slab with #3@8in to achieve an inelastic deflection of 3.17 inches.

1. The minimum flexural reinforcement that needs to be provided as per table 4-3 of UFC 3-340-02 is $1.875\ \sqrt{}f'_c/f_y\ bd = 1.875\ \sqrt{}4000 / 60000 \times 8 \times (2.81) = 0.04$ sq-in. Hence #3 rebar provided with $A_s = 0.11$ sq-in is okay.
2. The neutral axis depth $a = A_s f_{dv}/0.85bf'_{dc} = 0.11 \times 70200 / (0.85x\ 8x\ 4760) = 0.24$ inches. Hence the moment capacity $M_u = A_s f_{dv}/b \times (d-a/2) = 0.11x70200/8x\ (2.81-0.24/2) = 2600$ lbs.-in / in

3. Assuming the slab has one-way behavior with restraints not sufficient to prevent any rotation at ends, the ultimate resistance for unit width of slab, $r_u = 8(M_P)/L^2 = 8 \times (2600) / 58^2 = 6.2$psi.

4. Determination of modulus of elasticity and modular ratio:

$$E_c = w^{1.5}\, 33\, (f'c)^{1/2} = (150)^{1.5}\, (33)(4000)^{1/2} = 3835 \times 10^3 \text{ psi}$$

$$E_s = 29 \times 10^6 \text{ psi}$$

$$n = E_s / E_c = 29 \times 10^6 / 3835 \times 10^3 = 7.5$$

5. Determination of average moment of inertia for an inch width of slab:

$$I_g = 4^3/12 = 5.33 \text{ in}^4$$

$I_c = Fd^3$. With modular ratio n = 7.56 and reinforcement ratio $\rho = A_s/bd = 0.11/(8x3) = 0.0046$, F = 0.025 from figure 4-11 of UFC 3-340-02. Hence $I_c = 0.025 \times 2.81^3 = 0.55 \text{ in}^4$

$$I_a = (I_g+I_c)/2 = 2.94 \text{ in}^4$$

6. Equivalent elastic stiffness and deflection:

$$K_E = 384EI/5L^4 = 384x\ 3835x\ 10^3x\ 2.94 / (5x58^4) = 76.5 \text{ psi / in.}$$

The elastic deflection $X_E = r_u/K_E = 6.2 / 76.5 = 0.08$ inches.

7. Determination of natural time period:

Mass, m = $(150/12^3)$ pci x 4 inch x 1 inch / (32*12) in /sec^2 x 10^6 = 904 psi-msec^2/in

$K_{LM} = (0.78+0.66)/2 = 0.72$

$T_N = 2\,\pi\,\sqrt{}\,(m/K_E) = 2\,\pi\,\sqrt{}\,(0.72 \times 904 / 76.5) = 18.3$ msec

Duration of load T = 2 x 509 / 34 = 30 msec

8. Determination of pressure and impulse values:

For achieving 3.17 inches of maximum deflection observed in experiment, X_M/X_E = 3.17 / .08 = 39.6 and T/T_N = 30 / 18.3 = 1.64. From table 3-54, ru/P = 0.4, hence peak pressure P = 6.2 / 0.4 = 15.5 psi and corresponding impulse for a load duration of 30 msec = 0.5 x 30 x 15.5 = 232.5 psi-msec.

4.3. Comparison with Numerical Analysis and Design Results

The PI curves developed for RC slabs with #3@4in. and #3@8in. longitudinal reinforcement are compared with the experimental values and design values in this section. The PI curves developed for #3@4in. and #3@8in. longitudinal reinforcements in previous chapter are compared with the three experimental data points and one design data point as calculated in previous section. The comparisons are shown in figures 4-1 and 4-2 below. The experimental data points are shown as circles and the design example data point is shown as a star in figures 4-1 and 4-2. The PI curves with dashed lines correspond to SBEDS results and the PI curves with solid lines correspond to LS-DYNA results. The denotation for the damage levels for PI curves shown in figures 4-1 and 4-2 is same as described in chapter 3.

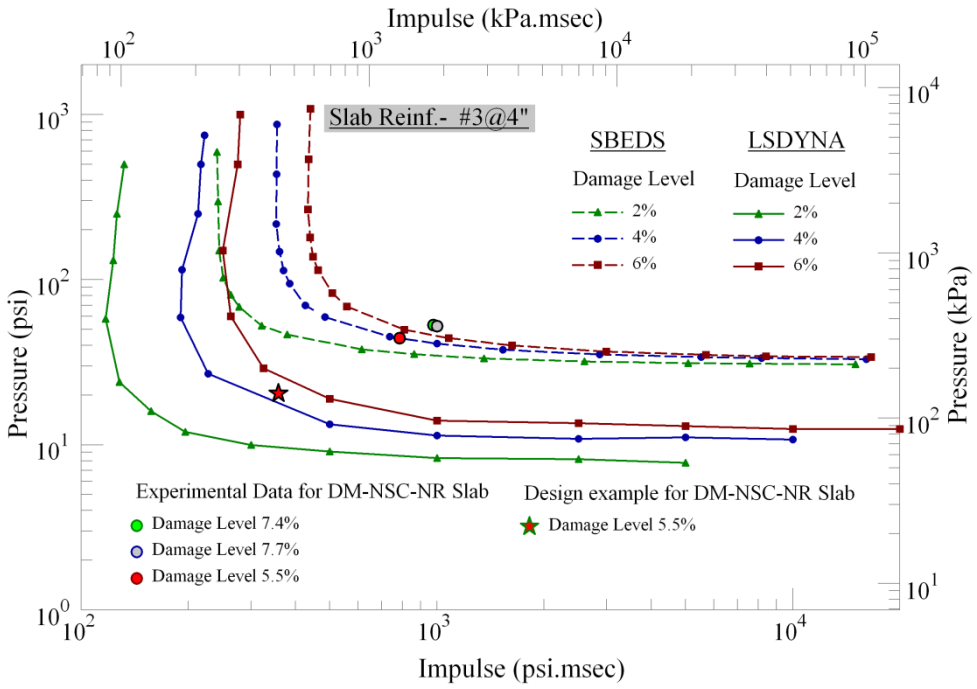

Figure 4-1: Comparison of PI curves for slab with ρ = 0.92%

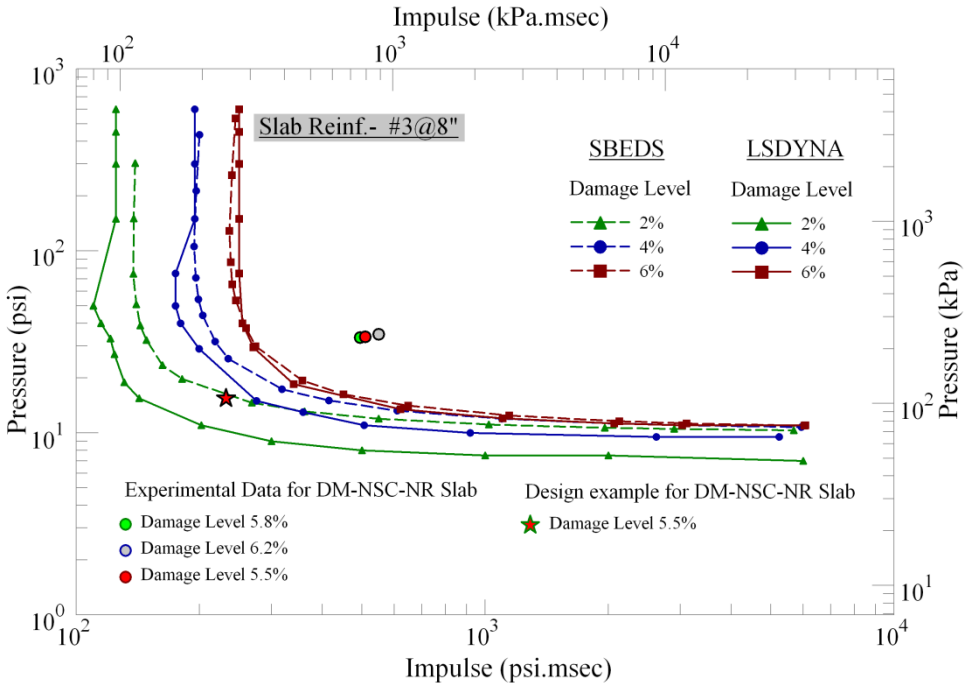

Figure 4-2: Comparison of PI curves for slab with ρ = 0.46%

4.4. Seismic Detailing for Blast resistance

It is important to review current seismic detailing practices and adopt relevant detailing for blast resistance because of three reasons: (1) several research studies have shown that seismic detailing will significantly improve blast resistance (2) a study by U.S Army Engineer Research and Development Center (ERDC) hypothetically strengthened Alfred P. Murrah Federal Building for high seismic demands. The building was severely damaged in a 1995 bombing and the damage included destruction of 42% of slabs. The blast and corresponding progressive collapse analyses showed that the pier-spandrel and special moment frame schemes would significantly reduce the amount of blast-induced damage and subsequent progressive collapse, compared with the response of the original building. Hence it can be concluded that seismic strengthening of the structural system will reduce demands on individual structural elements for blast scenario (3) it may be required to design a structural element or system to resist both blast and seismic forces in many cases. Hence it may be required to use the structural system and detailing that is most commonly used for building construction today.

4.4.1. Blast Loads vs. Seismic Loads

Blast loads are applied within a very short duration (fraction of a second) compared to seismic loads (which may last for several seconds). However, both seismic and blast resistant design approaches consider the time-varying nature of the loading function. The manner in which forces are distributed throughout the building is strongly affected by its configuration. While seismic forces are proportional to the mass of the building and increase the demand, inertial resistance plays a significant role in the design of structures to reduce

the response to blast loading. However, both these loadings are similar in context that they cause reversal of stresses in structural members due to change of their direction. During an earthquake a structure moves to and fro along a particular axis, whereas the blast pressure has positive and negative phases. On an element level, the plastic deformation demands for both seismically loaded structures and blast-loaded structures require attention to details. Many similar detailing approaches can be used to achieve the ductile performance of structural elements when subjected to both blast and seismic loading phenomenon.

4.4.2. Lateral Force Resisting Systems

The structural system usually consists of a combination of seismic and gravity load resisting frames in a structure. Designing all structural elements for seismic forces would not be economical due to stringent seismic detailing requirements as per detailing codes. Special reinforced concrete shear walls and special moment frames or a combination of both are commonly used lateral force resisting systems in reinforced concrete buildings. These lateral resisting systems are designed to resist the seismic forces on entire building. However, for blast scenario, it is important to evaluate the location of these lateral resisting systems as related to possible blast location and intensity. Usually, the exterior of building is most vulnerable to a blast scenario. Hence when designing a system to resist blast and seismic forces, it is important to location the seismic frames or shear walls on each perimeter side of the building.

4.4.3. Seismic Detailing of RC Slabs

The seismic detailing of reinforced concrete slab consists of four important aspects: (1) the slab reinforcement is hooked into available elements like walls or beams at slab perimeter ends (2) the slab diaphragm is provided with continuous chord reinforcement on the slab perimeter to provide for the in-plane bending of the slab (3) The reinforcement in divided into column and middle strips. The column strip is provided with more reinforcement (4) Reinforcement in column strip is provided with minimum Class B splicing and at least two rebar continuous through the column (ACI Committee 318 2008).

4.4.4. Blast Detailing of RC Slabs

The ductility of reinforced concrete slabs may be improved by using the following seismic detailing concepts of reinforced concrete slabs and walls (Austin et al. 2008). Improving the ductility of RC slabs can evidently improve the blast performance of RC slabs.

1) Provide chord reinforcement to resist lateral forces from an exterior wall due to blast loads
2) For thin slabs with one layer of reinforcement in each direction, provide at least 135 degree hook at rebar ends where it is not possible provide full anchorage.
3) Provide equal area of reinforcement in each direction. This will improve ductility and reduce enhancement of crack widths
4) Provide boundary elements for slabs with larger spans
5) Proportion maximum reinforcement ratio and slab thickness to ensure ductile failure mode

6) Provide compression reinforcement to provide ductility

4.5. Discussion of Results

The comparison of PI curves developed using numerical methods in Chapter 3 with experimental and design values calculated in previous sections is discussed here. The comparison is shown in figures 4-1 and 4-2 in previous sections.

As it can be seen from figure 4-1 for slab with #3@4in. longitudinal rebar, the experimental values lie above the PI curves developed using LS-DYNA which indicates that LS-DYNA approach is conservative for this slab. However the experimental data points are close to PI curves developed using SBEDS approach. The design example for the slab with #3@4in. longitudinal rebar as shown in previous section indicates that the design is conservative as compared to SBEDS analysis and experimental values but closely matches with LS DYNA analysis as shown in figure 4-1. Since all the SBEDS PI Curves are above the pressure and impulse values as calculated in design example for the slab, it is evident that SBEDS would show less than 2% damage for the same pressure and impulse values used in the design.

As it can be seen from figure 4-2 for slab with #3@8in. longitudinal rebar, the experimental values lie above the PI curves developed using both LS-DYNA and SBEDS which indicates that both the analysis approaches are conservative for this slab. It can be observed from figure 4-2 that the experimental pressure and impulse values would yield a much lower damage level when analyzed for the slab with #3@8in. longitudinal rebar using SBEDS and LS-DYNA. The design example data point also shows that the design is conservative as compared to both analysis and experimental values.

CHAPTER 5

CONCLUSIONS AND FUTURE WORK

The following conclusions can be drawn from the study performed on the response of the four types of reinforced concrete slabs subjected to blast loading

- Pressure-Impulse (PI) curves developed by using numerical simulations can be utilized to compare the resistance of different structures to blast loading. Four types of slabs whose difference is the longitudinal reinforcement size, spacing and ratio are compared.
- PI curves developed by using LS DYNA were observed to be typically conservative as compared to those developed using SBEDS.
- The difference between SBEDS and LS DYNA PI curves was typically observed to increase with increase in longitudinal reinforcement ratio.
- However, PI curves developed using SBEDS showed a much larger variation with change in reinforcement ratio as compared to PI curves developed using LSDYNA.
- The difference between PI curves developed using SBEDS and LSDYNA typically increased with damage level.
- The difference between PI curves developed using SBEDS and LSDYNA was more prominent in dynamic loading regime.
- SBEDS analysis also showed a significant improvement in blast resistance by decreasing the longitudinal reinforcement spacing with little variation in longitudinal reinforcement ratio. However, LS DYNA analysis did not show any significant difference due to variation in spacing of longitudinal rebar.
- SBEDS PI curves for slabs with ρ=0.92% and ρ =1.64% indicate a significant difference in the PI curves. However, LSDYNA PI curves for the slabs with ρ =0.92% and ρ =1.64% showed very little difference.
- The design of RC slabs per UFC 3-340-02 is typically conservative when compared with analytical (SBEDS and LSDYNA) and experimental results for the two slabs with ρ=0.46% and ρ=0.92%.

- The analytical results are typically conservative when compared with experimental results

Based on the research study conducted, the following recommendations are made for future research work on the blast analysis of RC slabs.

- Study the effect of varying the transverse reinforcement spacing on the blast resistance of RC Slabs
- Develop PI curves using SDOF analysis which includes both flexural and shear response
- Develop PI curves for a slab with different reinforcing using LSDYNA and compare with the curve fit equations developed in this research study
- Develop PI curves for varying slab thickness and spans
- Perform statistical analysis of PI curve data including all variables

APPENDIX A

TYPICAL MATERIAL INPUT AND OUTPUT FILE IN LS-DYNA

```
*MAT_WINFRITH_CONCRETE
$$$$$$$$$$$$$$$$$$$$$$$$$$$$$$$$$$$$$$$$$$$$$$$$$$$$$$$$$$$$$$$$$$$$$$$$$$$$$$$$
$                            Material Definitions
$#     mid        ro        tm        pr       ucs       uts        fe     asize
         1 2.2460E-4 3.6000E+6  0.180000 4000.0000 475.00000 2.0000E-4  0.125000
$#       e        ys        eh    uelong      rate      conm      conl      cont
     0.000     0.000     0.000     0.000  1.000000 -1.000000  0.025400  1.000000
$#    eps1      eps2      eps3      eps4      eps5      eps6      eps7      eps8
 -1.900E-5 -0.002000 -0.004000 -0.010000 -0.020000 -0.030000 -0.041000 -0.051000
$#      p1        p2        p3        p4        p5        p6        p7        p8
  1.330000  2.000000  4.000000  6.400000  8.000000 10.000000 12.600000 15.390000
```

Figure A-1: Concrete Material Properties used in Finite Element Analysis

```
*MAT_PLASTIC_KINEMATIC
$#     mid        ro         e        pr      sigy      etan      beta
         2 7.3000E-4 2.9000E+7  0.300000 60000.000     0.000     0.000
$#     src       srp        fs        vp
     0.000     0.000     0.000     0.000
```

Figure A-2: Reinforcing Steel Material Properties used in Finite Element Analysis

```
                                    messag
     Date: 11/14/2011      Time: 23:48:55

********  notice  ********  notice  ********  notice  ********
*                                                             *
* This is the LS-DYNA Finite Element code.                    *
*                                                             *
* Neither LSTC nor the authors assume any responsibility for  *
* the validity, accuracy, or applicability of any results     *
* obtained from this system. The user must verify his own     *
* results.                                                    *
*                                                             *
* LSTC endeavors to make the LS-DYNA code as complete,        *
* accurate and easy to use as possible.                       *
* Suggestions and comments are welcomed.  Please report any   *
* errors encountered in either the documentation or results   *
* immediately to LSTC through your site focus.                *
*                                                             *
* Copyright (C) 1990-2010                                     *
* by Livermore Software Technology Corp. (LSTC)               *
* All rights reserved                                         *
*                                                             *
********  notice  ********  notice  ********  notice  ********

Memory required to process keyword     :       957680
contracting memory to           1 end of keyword reader

LS-DYNA will perform a structural only analysis


S t o r a g e   a l l o c a t i o n

Memory required to begin solution      :      2182417
Additional dynamically allocated memory:       379939
                                 Total:      2562356

*** termination time reached ***

N o r m a l    t e r m i n a t i o n

S t o r a g e   a l l o c a t i o n

Memory required to complete solution   :      2182417
Additional dynamically allocated memory:       379943
                                 Total:      2562360

T i m i n g   i n f o r m a t i o n
                     CPU(seconds)   %CPU  Clock(seconds) %Clock
 ------------------------------------------------------------------
 ------------------------------------------------------------------
 T o t a l s           1.7876E+04  100.00     1.7875E+04  100.00

Problem time       =    2.0000E-01
Problem cycle      =     77300
Total CPU time     =     17876 seconds (   4 hours 57 minutes 56 seconds)
CPU time per zone cycle  =     25152 nanoseconds
Clock time per zone cycle=     25151 nanoseconds

Number of CPU's    1
NLQ used/max      96/   96
Start time   11/14/2011 23:48:55
End time     11/15/2011 04:47:46
Elapsed time   17931 seconds(  4 hours 58 min. 51 sec.) for   77300 cycles
```

Figure A-3: Typical Analysis Message File for Blast Analysis of RC Slab in LS-DYNA

APPENDIX B

TYPICAL INPUT DATA SHEET IN SBEDS

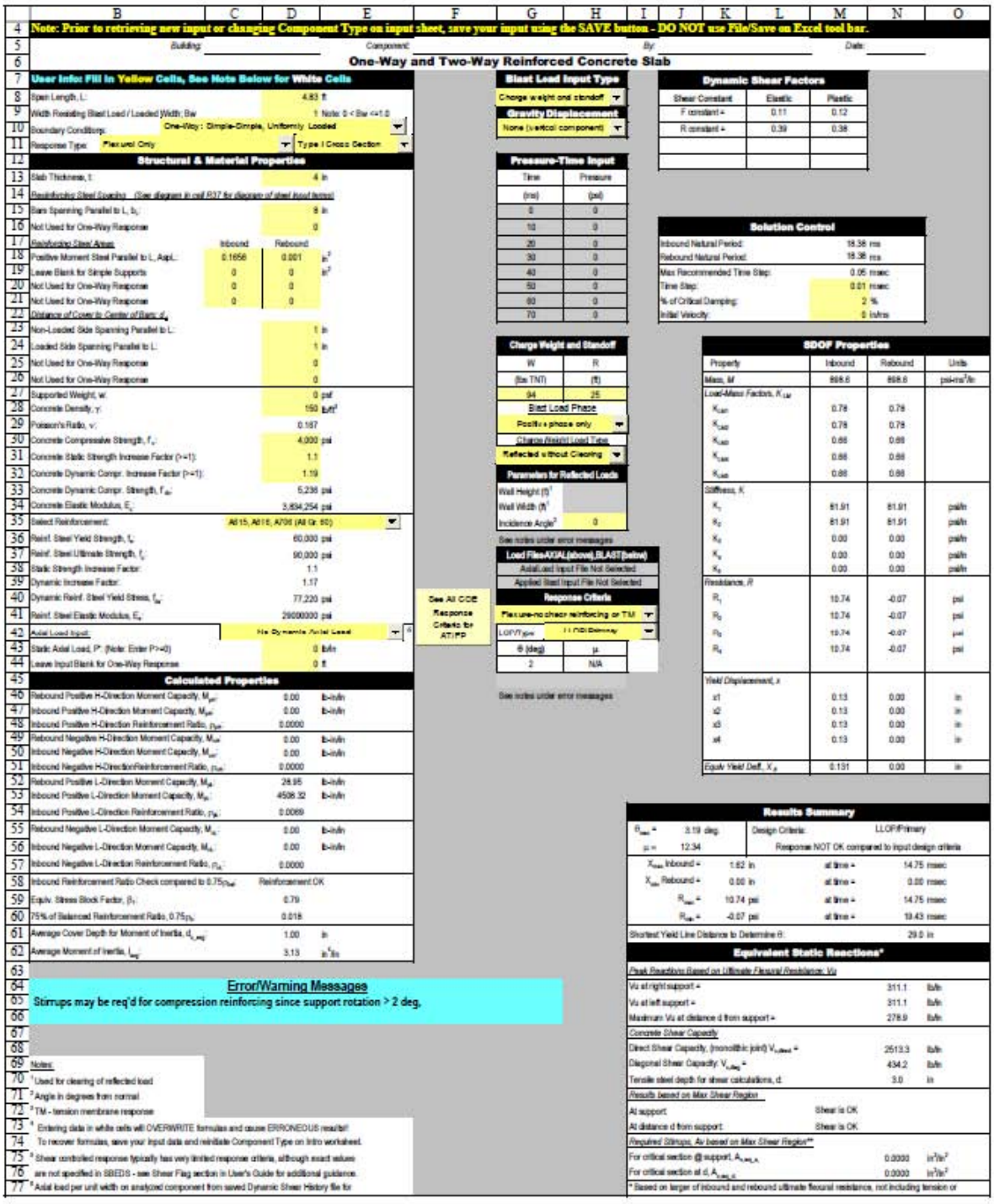

Figure B-1: SBEDS Input Data for RC Slab with ρ = 0.46%

REFERENCES

ACI Committee 318 (2008). "Building Code requirements for Structural Concrete (ACI 318-08) and Commentary(ACI318R-08)", Farmington Hills,MI:ACI

(Department of Defence), D. o. D. (2007). "Unified facilities criteria (UFC), DoD minimum antiterrorism standards for buildings". Department of Defense, UFC 4-010-01.

Agardh, L. (1997). "FE-Modelling of Fibre Reinforced Concrete Slabs Subjected to Blast Load." Journal De Physics **7**.

Austin D. Pan and Jack K P. Moehle (1992). "An Experimental Study of Slab Column Connections." Structural Journal **89**(6):626-638

Biggs, R., F. Barton, et al. (2000). "Finite Element Modeling and Analysis of Reinforced Concrete Bridge Decks." Report: Virginia Transportation Research Council.

Bogosian, D., J. Ferritto, et al. (2002). "Measuring uncertainty and conservatism in simplified blast models". Explosives Safety Seminar, Atlanta, Georgia.

Broadhouse, B. (1995). "The Winfrith Concrete Model in LS-DYNA3D." Report: SPD/D (95) **363**.

Criswell, M. E. (1972). "Design and Testing of a Blast-Resistant Reinforced Concrete Slab System", Department Technical Information Center (DTIC) Document.

El-Dakhakhni, W. W., W. F. Mekky, et al. (2010). "Validity of SDOF Models for Analyzing Two-Way Reinforced Concrete Panels under Blast Loading." Journal of Performance of Constructed Facilities **24**(4): 311-325.

Georgin, J. and J. Reynouard (2003). "Modeling of structures subjected to impact: concrete behaviour under high strain rate." Cement and Concrete Composites **25**(1): 131-143.

Hao, D. U. and L. Zhongxian (2008). "Numerical Analysis of Dynamic Behavior of RC slabs Under BLast Loading." Transactions of Tianjin University **15**(1): 61-64.

Hussein, A. T. (2010). "Non-Linear Analysis of SDOF System under Blast Load." European Journal of Scientific Research **45**(3): 430-437.

Jones, J., C. Wu, et al. (2009). "Finite difference analysis of simply supported RC slabs for blast loadings." Engineering structures **31**(12): 2825-2832.

Jorge O.Torres Alamo, S. D. R. (2008). "Dynamic Blast Load Simulator Micro-Alloy Vanadium Steel Reinforced Concrete Slab Experiments." US Army Corps of Engineers Research and Development Center.

Karthaus, W. and J. Leussink (1983). "Dynamic Loading: More Than Just a Dynamic Load Factor." Proceeding of the First International Symposium on the Interaction of Non-Nuclear Munitions with Structures,: 10-14.

Krauthammer, T. (1998). "Blast mitigation technologies: developments and numerical considerations for behavior assessment and design". International conference on structures under shock and impact computational mechanics Inc.

Krauthammer, T., S. Astarlioglu, et al. (2008). "Pressure-Impulse Diagrams for the Behavior Assessment of Structural Components." International Journal of Impact Engineering **35**(8): 771-783.

Krauthammer, T., M. Frye, et al. (2003). Advanced SDOF approach for structural concrete systems under blast and impact loads. 11th International Symposium on the Interaction of the Effects of Munitions with Structures Mannheim, Germany.

Krauthammer, T. and R. Otani (1997). "Mesh, gravity and load effects on finite element simulations of blast loaded reinforced concrete structures." Computers & Structures **63**(6): 1113-1120.

Kuang, X., X. Gu, et al. (2009). "Numerical Simulation for Responses of Reinforced Concrete Slabs under Blast Loads." Computational Structural Engineering: 691-698.

L.Agardh (1997). "FE-Modelling of Fibre Reinforced Concrete Slabs Subjected to Blast Load." Journal De Physics **7**.

Li, Q. and H. Meng (2002). "Pressure-impulse diagram for blast loads based on dimensional analysis and single-degree-of-freedom model." Journal of Engineering Mechanics **128**: 87.

Low, H. Y. and H. Hao (2002). "Reliability analysis of direct shear and flexural failure modes of RC slabs under explosive loading." Engineering structures **24**(2): 189-198.

LSDYNA_971 (2010). "Finite element modelling program for nonlinear dynamic analysis of the inelastic structures." Livermore Software Technology Corporation, CA, USA.

Mays, G. and P. D. Smith (1995). "Blast effects on buildings: Design of buildings to optimize resistance to blast loading", Thomas Telford, London.

Mlakar Sr, P., W. Corley, et al. (1998). "The Oklahoma City bombing: Analysis of blast damage to the Murrah Building." Journal of Performance of Constructed Facilities **12**: 113.

Morison, C. M. (2006). "Dynamic response of walls and slabs by single-degree-of-freedom analysis--a critical review and revision." International Journal of Impact Engineering **32**(8): 1214-1247.

Mosalam, K. M. and A. S. Mosallam (2001). "Nonlinear transient analysis of reinforced concrete slabs subjected to blast loading and retrofitted with CFRP composites." Composites Part B: Engineering **32**(8): 623-636.

Ottosen, N. S. (1977). "A failure criterion for concrete." Journal of the Engineering Mechanics Division.

Polcyn, M. A. and K. D. Myers (2010). Use of SBEDS for Blast Resistant Design in accordance with UFC 3-340-02, Defence Technical Information Center (DTIC) Document(http://www.dtic.mil/dtic).

Razaqpur, G. R. G., W. M. W. Mekky, et al. (2009). "Fundamental concepts in blast resistance evaluation of structures This article is one of a selection of papers published in the Special Issue on Blast Engineering." Canadian Journal of Civil Engineering **36**(8): 1292-1304.

Sangi, A. and I. May (2009). "High-Mass, Low-Velocity Impacts on Reinforced Concrete Slabs". 7th European LS-DYNA Conference.

SBEDS, U. S. A. C. o. E. P. D. C. (2008). "Single Degree of Freedom Blast Design Spreadsheet (SBEDS) Methodology Manual.". U.S. Army Corps of Engineers Protective Design Center Technical Report "PDC-TR 06-01 Rev1".

Schenker, A., I. Anteby, et al. (2008). "Full-scale field tests of concrete slabs subjected to blast loads." International Journal of Impact Engineering **35**(3): 184-198.

Schwer, L. (2011). "The Winfrith Concrete Model: Beauty of Beast? Insights into the Winfrith Concrete Model". 8th European LS-DYNA Users Conference, Strasbourg.

Smith, S. J., D. M. McCann, et al. (2009). Blast Resistant Design Guide for Reinforced Concrete Structures. Skokie,Illinois, Portland Cement Association.

Tanapornraweekit, G., N. Haritos, et al.(2007) "Modelling of a Reinforced Concrete Panel Subjected to Blast Load by Explicit Non-linear FE Code." Proceedings of the Earthquake Engineering in Australia conference2007.

TM5-1300. (1990). "Structures to Resist the Effects of Accidental Explosions", Joint Departments of the Army,Air Force and Navy, Washington D.C.

Wu, C., D. J. Oehlers, et al. (2009). "Blast testing of ultra-high performance fibre and FRP-retrofitted concrete slabs." Engineering structures **31**(9): 2060-2069.

Yuan, L., S. Gong, et al. (2008). "Spallation mechanism of RC slabs under contact detonation." Transactions of Tianjin University **14**(6): 464-469.

Zhou, X., V. Kuznetsov, et al. (2008). "Numerical prediction of concrete slab response to blast loading." International Journal of Impact Engineering **35**(10): 1186-1200.

Zineddin, M. and T. Krauthammer (2007). "Dynamic response and behavior of reinforced concrete slabs under impact loading." International Journal of Impact Engineering **34**(9): 1517-1534.

VITA

Jitesh Kumar Reddy Nalagotla was born in Hyderabad, India in 1976. He attended Indian Institute of Technology (IIT) Bombay, Mumbai, India for his Bachelor's degree in Civil Engineering. Following graduation he worked as a structural engineer for several years in India.

He joined the University of Missouri-Kansas City in spring semester 2011 to pursue his Masters in Civil Engineering with a focus on Structural Engineering. He was awarded graduate research assistantship from the Civil Engineering Department to study the Non-linear response of reinforced concrete structures subjected to blast loading and the evaluation of precast prestress concrete bridge approach Slabs for Missouri Department of Transportation. He is currently working on practical training as a structural engineer with Englekirk in Orange County, California.

He plans to utilize his research and educational knowledge and past professional experience in pursuing a career in Structural Engineering.